Environmental Management (2021) 68:240–261
https://doi.org/10.1007/s00267-021-01492-9

Evaluating the Effectiveness of Best Management Practices On Soil Erosion Reduction Using the SWAT Model: for the Case of Gumara Watershed, Abbay (Upper Blue Nile) Basin

Temesgen Gashaw[1] · Yihun T. Dile[2] · Abeyou W. Worqlul[3] · Amare Bantider[4,5] · Gete Zeleke[4] · Woldeamlak Bewket[4,6] · Tena Alamirew[4,7]

Received: 8 January 2021 / Accepted: 29 May 2021 / Published online: 8 June 2021

Abstract

This study was conducted to evaluate the effectiveness of best management practices (BMPs) to reduce soil erosion in Gumara watershed of the Abbay (Upper Blue Nile) Basin using the Soil and Water Assessment Tool (SWAT) model. The model was calibrated (1995–2002) and validated (2003–2007) using the SWAT-CUP based on observed streamflow and sediment yield data at the watershed outlet. The study evaluated four individual BMP Scenarios; namely, filter strips (FS), stone/soil bunds (SSB), grassed waterways (GW) and reforestation of croplands (RC), and three blended BMP Scenarios, which combines individual BMPS of FS and RC (FS & RC), GW and RC (GW & RC), and SSB and GW (SSB & GW). Mean annual sediment yield at the baseline conditions was estimated at 19.7 t $ha^{-1}yr^{-1}$, which was reduced by 13.7, 30.5, 16.2 and 25.9% in the FS, SSB, GW, and RC Scenarios, respectively at the watershed scale. The highest reduction efficiency of 34% was achieved through the implementations of the SSB & GW Scenario. The GW & RC, and FS & RC Scenarios reduced the baseline sediment yield by 32% and 29.9%, respectively. The study therefore concluded that the combined Scenarios mainly SSB & GW, and GW & RC can be applied to reduce the high soil erosion in the Gumera watershed, and similar agro-ecological watersheds in Ethiopia. In cases where applying the combined scenarios is not possible, the SSB Scenario can yield significant soil erosion reduction.

Keywords Best management practices · Modeling · Scenarios · Water-induced soil erosion

Introduction

Soil erosion is one of a pressing global environmental problem (Pimentel and Burgess 2013; Blanco and Lal 2008; Pimentel 2006). A global estimate indicates that by mid-1990s, soil degradation affected around two billion hectares of cultivated land (i.e., about one-third of total cultivated land), of which water-induced soil erosion accounted for about 56% (Oldeman et al. 1995). With respect to severity, studies (e.g., Lal 1994; Speth 1994) indicated that ~80% of the world's cultivated lands are affected by moderate to severe rate of water-induced soil erosion. This resulted in loss of ~10 million ha of croplands worldwide (Pimentel 2006). Soil erosion is a serious challenge particularly in Africa, Asia, and Latin America, where the highest number of their populations relying on agriculture for livelihoods (Pimentel and Burgess 2013; Awulachew et al. 2008; Blanco and Lal 2008). In fact, compared to Asia and Latin America, the effects of soil erosion are grave in Africa.

✉ Temesgen Gashaw
gtemesgen114@gmail.com

[1] Department of Natural Resource Management, College of Agriculture and Environmental Science, Bahir Dar University, Bahir Dar, Ethiopia

[2] College of Agriculture and Life Sciences, Texas A&M University, College Station, TX, USA

[3] Blackland Research and Extension Center, Texas A & M University, Temple, TX, USA

[4] Water and Land Resource Center, Addis Ababa University, Addis Ababa, Ethiopia

[5] College of Development Studies, Addis Ababa University, Addis Ababa, Ethiopia

[6] Department of Geography and Environmental Studies, Addis Ababa University, Addis Ababa, Ethiopia

[7] Ethiopiann Institute of Water Resources, Addis Ababa University, Addis Ababa, Ethiopia

Of the 1 billion people affected by soil erosion globally, 50% are found in Africa, which underscores the severity of the problem in the African continent (Blanco and Lal 2008).

Soil erosion is causing extreme onsite (e.g., loss of fertile soil and crop productivity) and offsite (sedimentation of water infrastructures) negative externalities (Gashaw et al. 2019; Nyssen et al. 2007a, 2007b; Sonneveld and Keyzer 2003; Zeleke 2000), particularly in the highland regions of Ethiopia due to its rugged topography and intense rainfall (Gashaw et al. 2020; Hurni et al. 2005; Reusing et al. 2000). For example, a recent research showed that the mean annual soil erosion rate in a watershed that is located in the northwestern Ethiopian highlands is 55 t $ha^{-1}yr^{-1}$ (Gashaw et al. 2019). Other studies in the Ethiopian highland showed a higher estimate. For example, Yihenew and Yihenew (2013) reported that mean annual soil loss rate in Harefetay watershed may reach up to 84 t ha^{-1} yr^{-1}. While Zeleke (2000) reported that the mean spatio-temporal annual soil loss in Dembecha area is 243 t ha^{-1} yr^{-1}. As a result, soil erosion caused loss of ~1.5 billion tons of topsoil every year from the Ethiopian highland, which could have helped producing 1.5 million tons of grains (Taddese 2001).

Besides the land degradation in the highlands of Ethiopia (Gebremicael et al., 2013; Ahmed and Ismail, 2008; Awulachew et al. 2008), soil erosion is causing downstream sedimentation problems to several water supply and hydropower generating reservoirs (Wolancho 2012; Awulachew et al. 2008; Ahmed and Ismail, 2008). For example, the Sinnar dam in Sudan, which is located downstream of the Upper Blue Nile Basin, lost 71% of its storage capacity within 61 years due to sedimentation. A large part of the sedimentation of this dam (~43%) occurred in just 5 years (i.e., between 1981 and 1986) (Awulachew et al. 2008; Ahmed and Ismail, 2008). Likewise, the Khashm ElGirba and Rosieres reservoirs, which are further located downstream of the Upper Blue Nile Basin in Sudan, lost about 50 and 36% of their planned storage capacities during the 1964–1977 and 1964–1992 periods, respectively (Awulachew et al. 2008; Ahmed and Ismail, 2008). Similar sedimentation problems were observed in the water supply and hydropower generation reservoirs of Ethiopia (Temesgen et al. 2013; Wolancho 2012; Setegn et al. 2009; Yohannes, 2005). Some of the affected lakes that are under serious threats due to soil erosion are Lake Abijata in the Central Rift Valley region (Temesgen et al. 2013) and Lake Tana in the northern highlands (Lemma et al. 2018; Setegn et al. 2009).

Such serious soil erosion and sedimentation problems in the highlands of Ethiopia urges implementation of agricultural BMPs that are vital to reduce soil erosion and thereby lessen rate of land degradation and filling up of reservoirs (Briak et al. 2019; Himanshu et al. 2019; Park et al. 2014; Bosch et al. 2013; Betrie et al. 2011). Globally, several studies evaluated the effectiveness of BMPs to reduce sediment load and agricultural nutrients to freshwater ecosystems (e.g., Uniyal et al. 2020; Briak et al. 2019; Park et al. 2014; Bosch et al. 2013; Arabi et al. 2008). However, majority of these studies were undertaken in North America (e.g., Lamba et al. 2016; Bosch et al. 2013; Arabi et al. 2008), Europe (e.g., López-Ballesteros et al. 2019; Engebretsen et al. 2019; Lam et al. 2011) and Asian continents (e.g., Uniyal et al. 2020; Himanshu et al. 2019; Park et al. 2014). There are only few studies that evaluate BMPs in Africa (e.g., Briak et al. 2019 in Morocco; Gathagu et al. 2018 in Kenya; Betrie et al. 2011 in Ethiopia). The existing limited studies in the continent were focused on the evaluation of only certain numbers of individual BMPs such as terracing, contouring and strip-cropping in Kalaya River Basin, Morocco (Briak et al. 2019) and terracing and grassed waterways (GW) in Thika-Chania catchment, Kenya (Gathagu et al. 2018). Furthermore, the calibration and validation of the models in these studies was not using observed sediment data as there is limited continuously monitored sediment data. As a result, calibration and validation of models in the existing few studies were undertaken through establishing a single sediment rating curve (e.g., Aga et al. 2018; Asres and Awulachew 2010) or using the available few measured sediment concentration data only (e.g., Briak et al. 2019; Betrie et al. 2011). Developing a single sediment rating curve with high numbers of sediment data from either wet or dry season may introduce uncertainties in the model's prediction unless the collected sediment data in dry and wet seasons are proportional. Therefore, calibration and validation of models using such sediment concentration data will not be sufficient and pose uncertainty.

Correspondingly, limited studies exist in Ethiopia that evaluated impacts of BMPs on soil erosion and other non-point source pollutions. Most of these studies are undertaken on the Lake Tana basin (e.g., Lemma et al. (2019), its watersheds (Asres and Awulachew 2010) or the Upper Blue Nile Basin (Betrie et al. 2011). In addition, previous studies assessed the implementation of single BMPs, and considered limited BMP options. For instance, Asres and Awulachew (2010) studied the effects of different filter strips (FS) at the Gumera watershed. On the other hand, Lemma et al. (2019) assessed the effectiveness of grass strips, stone/soil bunds (SSB), *Acacia decurrens*-based crop rotation, zero grazing and reforestation in the Lake Tana Basin where Gumera watershed is located. In the Upper Blue Nile Basin, Betrie et al. (2011) showed satisfactory sediment reduction with implementations of FS, SSB and reforestation. Furthermore, previous studies (e.g., Asres and Awulachew 2010; Betrie et al. 2011) were used a coarser resolution (90 m) Digital Elevation Model (DEM) while DEM's resolution has an impact on the representation of

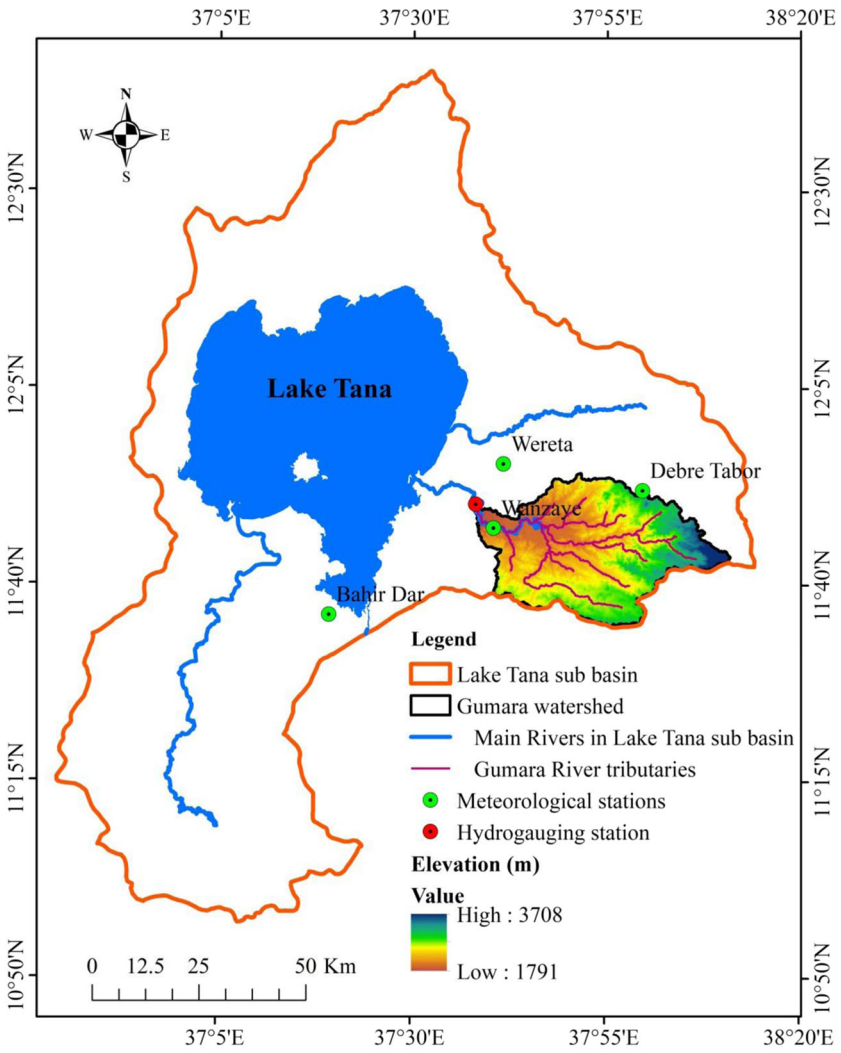

Fig. 1 Location map of Gumara watershed from Lake Tana sub basin

terrain morphology (e.g., total number of channels, their length and hierarchy, etc) and thereby affect hydrological and sediment yield predictions (Zhang et al. 2008; Rocha et al. 2020).

This research has been undertaken in Gumara watershed, which is one of the agricultural productive areas in the highlands of Ethiopia. However, the watershed has been experiencing severe soil erosion due to extensive agricultural practices and extreme rainfall storms (Asres and Awulachew 2010). The high sediment load from the upstream tributaries has been a treat to Lake Tana, which is the source of the Upper Blue Nile River in which the Grand Ethiopian Renaissance Dam (GERD) is under construction. For example, water hyacinth has been expanding in the Lake Tana since 2011 (Anteneh et al. 2014). Studies indicated that high rate of sediment load to the Lake contributed a fertile ground for the water hyacinth expansion (Dersseh et al. 2019). Unless the high water-induced erosion in the Lake Tana watersheds is abated, Lake Tana, GERD and other reservoirs will be filled with sediment at an alarming rate. This study, therefore, studied the effectiveness of individual and combined BMPs to reduce soil erosion in Gumara watershed using the Soil and Water Assessment Tool (SWAT). SWAT was chosen due to its demonstrated performance in simulating sediment yield and evaluating effects of BMPs across different scales of watersheds (Uniyal et al. 2020; Briak et al. 2019; Himanshu et al. 2019; Park et al. 2014; Bosch et al. 2013; Betrie et al. 2011).

Materials and Methods

Descriptions of the Study Area

The study was conducted in the Gumara watershed, which covers ~1250 km^2 in the Upper Blue Nile Basin of Ethiopia (Fig. 1). Geographically, the watershed is located between 11°35′–11°55′ N and 37°35′–38°10′ E. The elevation of the

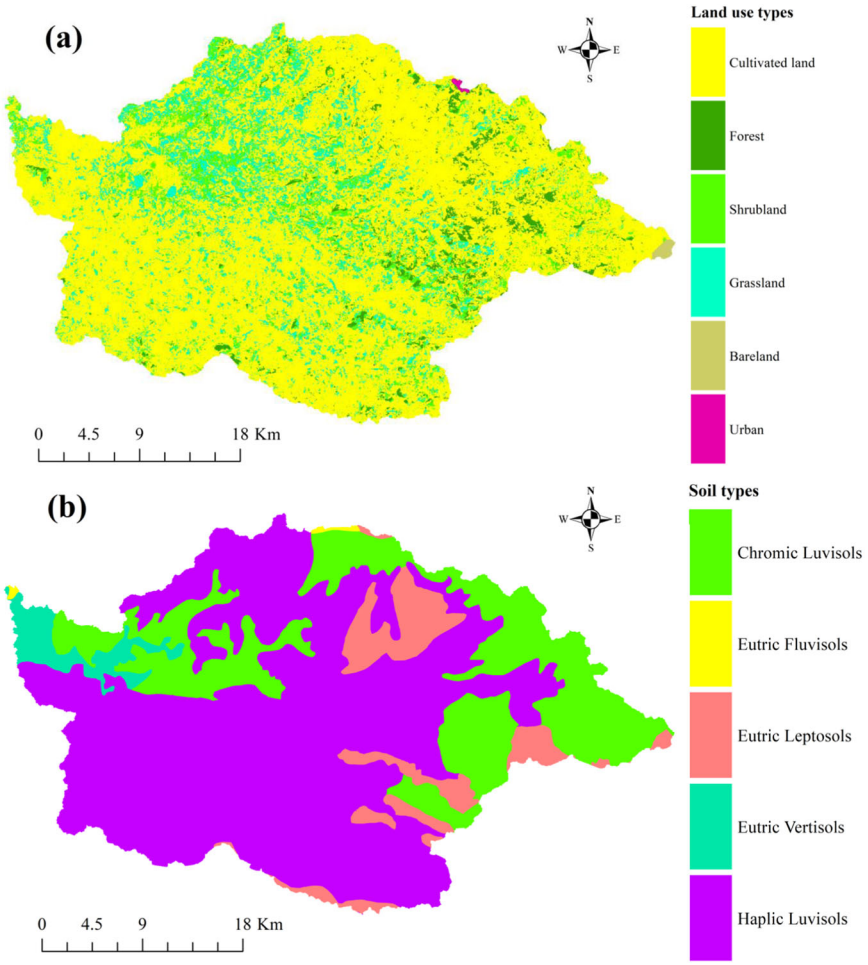

Fig. 2 The land use (**a**) and soil type (**b**) maps of the study area

watershed ranges from 3708 m above sea level (m a.s.l) to 1791 m a.s.l with a mean elevation of 2263 m a.s.l (Fig. 1). Gumara River is one of the main Rivers flowing into Lake Tana (Fig. 1). The dominant land uses in the watershed are cultivated land, grassland, shrubland, and forest land (Fig. 2). Agriculture in the watershed includes both rain-feed and irrigated agriculture.

In the watershed, there are two main seasons, namely: a rainy season which extends from June to September which is locally called *Kiremt* and a dry season which extends from October to May, locally called *Bega*. Based on observed climate data in four climate stations (i.e., Bahir Dar, Wanzaye, Wereta and Debre Tabor) (Fig. 1), the annual rainfall for the period 1995–2007 varies between 1481 mm $year^{-1}$ (Debre Tabor station) and 1267 mm $year^{-1}$ (Wereta station). The annual rainfall of Wanzaye and Bahir Dar stations during these periods was 1421 mm $year^{-1}$ and 1383 mm $year^{-1}$, respectively (NMSA 2019). The long term mean of maximum and minimum annual temperature of the four meteorological stations was 27 °C and 12 °C, respectively (NMSA 2019).

SWAT Data Inputs

SWAT is a continuous semi-distributed model that was developed in the 1990s to evaluate impacts of agricultural practices on water, sediment, and agricultural chemical contaminants in complex watersheds with variable conditions (Arnold et al. 1998, 2012). The model requires spatial (i.e., DEM, land use, and soil maps) and temporal (climate) data to simulate different biophysical processes. Moreover, streamflow and sediment data are needed for model calibration and validation.

Spatial data

The DEM was used to create slope map and discretize stream networks, sub basin and watershed characteristics including HRUs creations. The DEM data was obtained from Shuttle Radar Topography Mission (SRTM 2019), and it has a spatial resolution of 30 m.

The land use map was prepared from cloud free 30 m resolutions Landsat_7 ETM (Path/row 169/52, date 13 January 2001) (USGS 2019). The time of the selected

Table 1 Evaluation of image classification

	Reference from Google earth (Date: 16 January 2001)							
	Cultivated	Forest	Shrubland	Grassland	Bareland	Urban	Row Total	User Acc.
Classification result (Date: 13 January 2001)								
Cultivated	**82**	0	0	5	1	1	89	92.1
Forest	0	**78**	4	1	0	0	83	94.0
Shrubland	0	7	**61**	2	0	0	70	87.1
Grassland	5	0	3	**75**	2	1	86	87.2
Bareland	3	0	0	1	**32**	1	37	86.5
Urban	2	0	0	1	2	**23**	28	82.1
Column Total	92	85	68	85	37	26	393	
Prod Acc.	89.1	91.8	89.7	88.2	86.5	88.5		
	Kappa coefficient = 0.87				Overall accuracy = 89.3%			

Note that the bold numbers are the correctly classified values

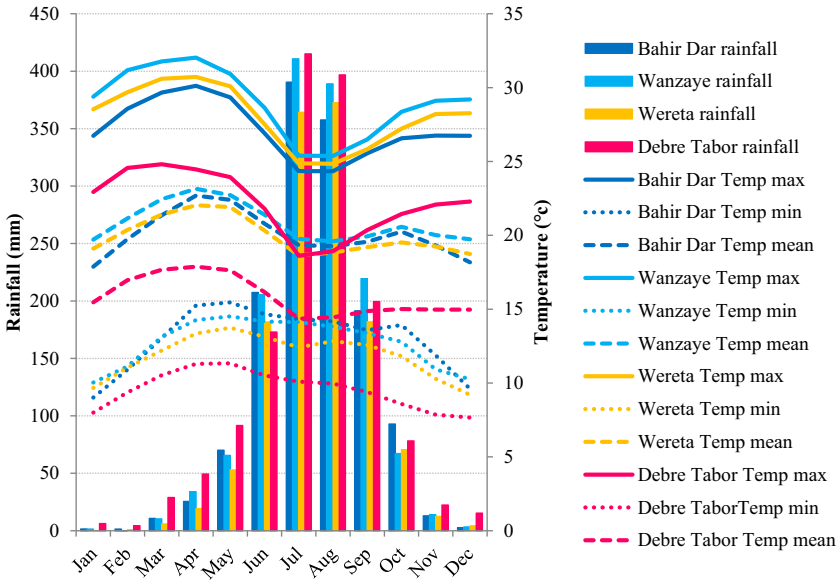

Fig. 3 The monthly rainfall and temperature (1995–2007) features of the four meteorological stations

image is within the observed climate, streamflow and sediment records to ensure consistent simulation results. Thematic information from the image was extracted applying supervised classification technique with Maximum Likelihood Classification algorithm in ERDAS Imagine 2014. Training points for image classification and validations were collected from each land use types from the Google Earth Image (i.e., 16 January 2001). Discussions with elder people were also undertaken to classify and verify the image analysis. The accuracy of the classified image was assessed with reference to the corresponding Google earth image. The classification result showed that an overall accuracy of 89.3% and a Kappa coefficient of 0.87 (Table 1), which suggested a very good image classification performance (Monserud 1990).

The identified land use classes are cultivated land, forest, shrubland, grassland, bareland and urban (Fig. 2a). The cultivated land is found as the dominant land use type, which accounts 75.6% of the watershed. Grassland, shrubland and forest covered 12.1%, 8.1% and 3.9%, respectively. Bareland and urban land use types were found minor land use types in the watershed representing only 0.2% and 0.1%, respectively.

Soil map was another important spatial input to the SWAT model, which is used to define HRUs and provide different soil phyio-chemical properties. There are five soil types in Gumara watershed, namely Haplic Luvisols (63.4%), Chromic Luvisols (25%), Eutric Leptosols (8.2%), Eutric Vertisols (3.2%), and Eutric Fluvisols (0.2%). The spatial map of the soil data was obtained from the hydrology department of Ministry of Water, Irrigation and Electricity (MoWIE 2019). In addition, soil textural classes and organic carbon content of the soil types for three soil layers (i.e., 0–30, 30–100 and 100–200 cm) were collected from the International Soil Reference Information Center (ISRIC) database (Hengl et al. 2017). Saxton and Rawls (2006)

pedotransfer function was used to calculate the detailed soil physiochemical properties required by the SWAT model using the collected soil data from the ISRIC database. Regarding the soil depths, which is one of the required data for the three soil layers, this study assigned soil depths for each soil types from Worqlul et al. (2018), which is a very detailed study in the same watershed on the response of hydrological components to soil characteristics.

Temporal data

SWAT requires continuous long term climate data, such as precipitation, temperature (maximum and minimum), wind speed, solar radiation and relative humidity. Daily records of these climate data at four stations for 1993–2007 were collected from the Ethiopian National Meteorological Services Agency (NMSA 2019). The four meteorological stations are Bahir Dar, Wanzaye, Wereta and Debre Tabor (Fig. 1). A weather generator that helps to complete missing records was prepared using SWAT's Weather Generator Parameters Estimation Tool. The monthly mean precipitation and temperature characteristics of the four meteorological stations during 1995–2007 are shown in Fig. 3.

Measured streamflow and sediment data are the other temporal data needed for hydrological modeling during the SWAT-CUP simulation. Model calibration and validation were undertaken using observed streamflow and sediment data that are collected at Gumara gauging station (Fig. 1) for 13 years (1995–2007). The streamflow and sediment data were obtained from MoWIE (2019). The sediment data obtained from MoWIE (2019) was not a continuous record. Consequently, continuous sediment data at daily basis at Gumara gauging station was obtained through establishing a relationship of the available streamflow and sediment data through a sediment rating curve for wet (June–September) and dry (October–May) seasons (Fig. 4). The estimated daily sediment values were aggregated into monthly data to calibrate the model on the monthly time step.

Model Setup

A drainage threshold area of 2500 ha was used to capture the actual river system in the watershed. This threshold area subdivided the studied watershed into 24 sub basins. The hydrological response units (HRUs) were defined by combining the slope, land use and soil maps using multiple HRUs options, in which more than one HRUs were created within a sub basin. A 20% (land use), 10% (soil) and 10% (slope) thresholds were used to define the HRUs, which provided a reasonable number of HRUs that gave satisfactory streamflow estimation in Gumara watershed. These land use-soil-slope combinations means land uses, soils and slope ranges whose areas are less than these thresholds of

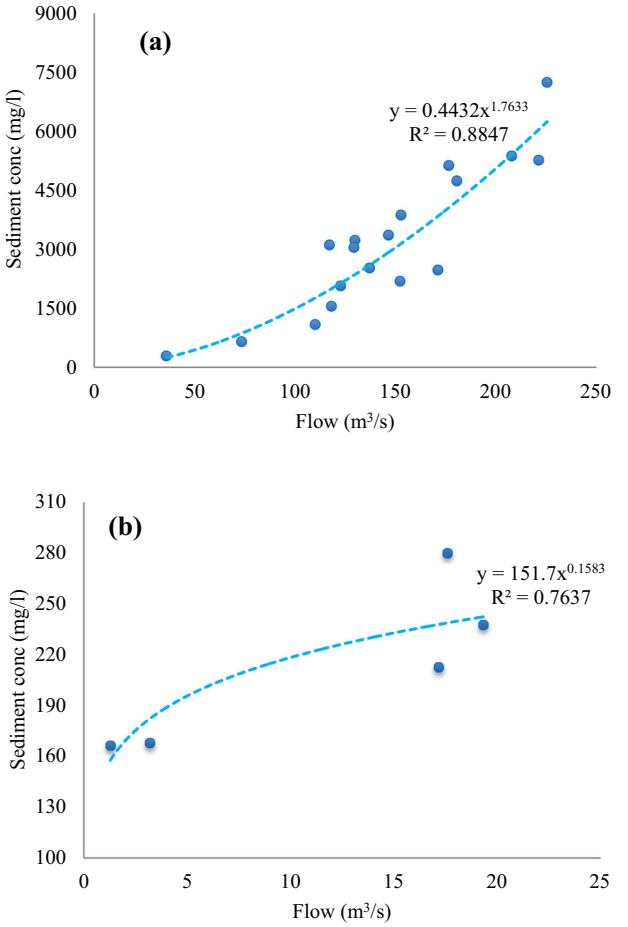

Fig. 4 The discharge-sediment rating curves of Gumara watershed for wet (**a**) and dry (**b**) seasons

the sub basin area are eliminated from HRU formation within each sub basin. The eliminated areas were distributed proportionally to the remaining units of slope, land use or soil features. Forest, shrubland, bareland and urban land use types were exempted from the land use threshold eliminations since they have a smaller representation in the watershed. The slope map was classified into 0–5, 5–15 and >15% to setup the model in such a way that BMPs will be implemented according to slope recommendations (Dile et al. 2016). Such HRU definition resulted in 392 HRUs.

Surface runoff was simulated using the Soil Conservation Service (SCS) curve number (CN) method (USDA-SCS 1972). The Penman-Monteith method, which requires precipitation, temperature, solar radiation, relative humidity and wind speed data, was applied to estimate Potential evapotranspiration (PET). Simulation of flow of water in the channels was made with a variable storage routing method. Sediment yield was predicted for each sub basins and HRUs based on the Modified Universal Soil Loss Equation (Williams 1995). In this study, the ArcGIS interface of SWAT (ArcSWAT 2012) was used for hydrology and sediment simulations.

Table 2 List of streamflow and sediment parameters considered for calibration and validation of SWAT and parameters space that are used for the initial model run

Flow/Sediment	Parameter	Description	Parameter space
Streamflow	r__CN2.mgt	SCS runoff curve number	−0.1–0.1
	v__ALPHA_BF.gw	Baseflow alpha factor (days)	0–1
	v__GW_DELAY.gw	Groundwater delay (days)	0–300
	v__GWQMN.gw	Threshold depth of water in the shallow aquifer requiredfor return flow to occur (mm)	0–4500
	v__GW_REVAP.gw	Groundwater "revap" coefficient	0.02–0.17
	v__ESCO.hru	Soil evaporation compensation factor	0.35–0.95
	v__REVAPMN.gw	Threshold depth of water in the shallow aquifer for "revap"to occur (mm)	0–400
	r__SOL_AWC.sol	Available water capacity of the soil layer	−0.1–0.1
	v__CH_K2.rte	Effective hydraulic conductivity in main channel alluvium	5–130
	v__CH_N2.rte	Manning's "n" value for the main channel	0.01–0.3
Sediment	v_SPCON.bsn	Linear parameter for calculating the maximum amount of sediment that can be re-entrained during channel sediment routing	0.0001–0.01
	v_SPEXP.bsn	Exponent parameter for calculating sediment re-entrained in channel sediment routing	1–1.5
	v_CH_COV1.rte	Channel erodibility factor	−0.05–0.4
	v_CH_COV2.rte	Channel cover factor	−0.001–0.6
	v_USLE_P.mgt	USLE support practice factor	0–1
	v_USLE_C{AGRC}.plant.dat	Min value of USLE C factor for land cover	0.003–0.5
	v_USLE_C{FRST}.plant.dat	Min value of USLE C factor for land cover	0.001–0.5
	v_USLE_C {RNGE}.plant.dat	Min value of USLE C factor for land cover	0.001–0.5
	v_USLE_C {RNGB}.plant.dat	Min value of USLE C factor for land cover	0.001–0.5

Note that "r_" represents adding 1 from the fitted value and multiply the result with the parameters initial value; "v_" indicates changing the initial value with the fitted value; "a_" indicates adding the fitted value to the initial model value

ARRC Cultivated land, *FRST* Forest, *RNGE* Grassland, *RNGB* Shrubland

Sensitivity Analyses, and Model Calibration and Validation

Sensitivity analyses were undertaken considering 10 streamflow and 9 sediment parameters (Table 2) using expert judgment and from previous studies in the study region (Worqlul et al. 2018; Lemma et al. 2019; Dile et al. 2016; Setegn et al. 2010, 2008). Sensitivity analyses were made in SWAT-CUP 2012 version 5.1.6.2 using global sensitivity analysis that allows changing each parameter at a time (Arnold et al. 2012; Abbaspour, 2014). Indices such as t-Stat to measure the sensitivity of each parameter and *P* value to provide the significance of sensitivity were used. According to Abbaspour (2014), the higher absolute values of *t*-test indicate a parameter's high sensitivity, and it is most significant when *p* value is 0.

Calibration and validation were initially made for streamflow followed by calibration and validation of sediment. The streamflow and sediment data were available for the period 1995–2007 in which the data from 1995–2002 to 2003–2007 were used for calibration and validation, respectively. The data from 1993 to 1994 were used for model warm up, which helps to initialize biophysical processes in the model. These length of streamflow and sediment records were chosen considering the availability of quality observed data records. A monthly time step calibration and validation were carried out using SWAT-CUP 2012 version 5.1.6.2 in SUFI-2 algorithm (Abbaspour, 2014). The selection of the monthly simulation period is based on the suggestion of Moriasi et al. (2007), which indicated that calibrating models at monthly time step is sufficient for water balance and impact studies. Evaluating the SWAT model performance at

Table 3 Performance ratings of SWAT for a monthly based simulation (Moriasi et al. 2007)

Performance rating	NSE	PBAIS (%)		RSR
		Streamflow	Sediment	
Very good	$0.75 < NSE \le 1.00$	$PBIAS < \pm 10$	$PBIAS < \pm 15$	$0.00 \le RSR \le 0.50$
Good	$0.65 < NSE \le 0.75$	$\pm 10 \le PBIAS < \pm 15$	$\pm 15 \le PBIAS < \pm 30$	$0.50 < RSR \le 0.60$
Satisfactory	$0.50 < NSE \le 0.65$	$\pm 15 \le PBIAS < \pm 25$	$\pm 30 \le PBIAS < \pm 55$	$0.60 < RSR \le 0.70$
Unsatisfactory	$NSE \le 0.50$	$PBIAS \ge \pm 25$	$PBIAS \ge \pm 55$	$RSR > 0.70$

daily and monthly time steps in the three watersheds of the Lake Tana Sub Basin (i.e., Gilegel Abay, Gumara and Rib watersheds), Tigabu et al. (2019) reported that the model is generally better in the monthly time step simulations.

The SWAT model was evaluated using the suggested performance measure statistics by Moriasi et al. (2007) (Table 3). These are Nash-Sutcliffe Efficiency (NSE), Percent Bias (PBIAS) and Root Mean Square Error (RMSE)-observations standard deviation ratio (RSR). NSE is a standardized statistics that defines the relative magnitude of the residual variance compared to the measured data variance. PBIAS accounts for the estimation bias of the model to be larger or smaller than the observations. RSR standardizes the RMSE using the observation standard deviations. In addition, coefficient of determination (R^2) (Begou et al. 2016) was used to evaluate consistency of simulated and observed streamflow and sediment data.

BMPs Scenarios

SWAT is one of the widely implemented hydrological models to evaluate effectiveness of BMPs in relation to sediment load/yield and agricultural non-point source pollutants reduction in many areas of the world. For example, the model was extensively applied in North America such as in Lake Erie watersheds (Bosch et al. 2013), Pleasant Valley watershed (Lamba et al. 2016) and Upper East River watershed (Merriman et al. 2019). SWAT was also widely implemented to evaluate efficiency of several BMPs in Asia such as Marol watershed, India (Himanshu et al. 2019) and Chungju dam watershed, South Korea (Park et al. 2014) and Europe such as in El Beal watershed, Spain (López-Ballesteros et al. 2019) and Kielstau catchment, Germany (Lam et al. 2011). The model was also effectively implemented in Africa such as Kalaya River Basin, Morocco (Briak et al. 2019) and Thika-Chania catchment, Kenya (Gathagu et al. 2018). In Ethiopia, this physically based hydrological model was applied in Lake Ziway Basin (Aga et al. 2018), Lake Tana sub basin (Lemma et al. 2019), Upper Blue Nile Basin (Betrie et al. 2011) and Gumera watershed (Asres and Awulachew 2010) with the aim of evaluating effects of certain BMPs in relation to sediment yield reduction.

In this study, after SWAT calibration for streamflow and sediment parameters, effectiveness of four independent and three combined BMPs in reducing sediment yield were evaluated against the baseline condition. The individual BMP Scenarios considered were FS (FS Scenario), SSB (SSB Scenario), GW (GW Scenario) and reforestation of croplands (RC Scenario). While the blended BMPs were a combination of FS and RC (FS & RC Scenario), integrating GW and RC (GW & RC scenario) and implementing SSB and GW together (SSB & GW Scenario). The details of the considered BMP Scenarios are given below.

The baseline condition is the existing state in the watershed. Hence, the sediment yield obtained after calibration of streamflow and sediment is represented as the baseline condition.

The first scenario, filter strip scenario (Scenario FS), is considered due to the fact that establishing vegetation such as grasses along the cropland contours helps to slow down the speed of runoff, minimize sheet and rill erosion, enhance infiltration and baseflow, and improve sediment trapping (Betrie et al. 2011). Hence, FS reduce development of erosional landscape process (e.g., rills and gullies) and enhances formations of depositional land forms. This soil and water management practice can be implemented in many areas of the Ethiopian highlands to reduce the high soil erosion rates and sediment yields and hence reduce siltation of water supply and power generating reservoirs (Lemma et al. 2019; Demissie et al. 2013; Betrie et al. 2011). Several local grasses are available in the study region (northwestern Ethiopia) for this purpose (Mekonnen et al. 2016). To assess effects of applying Scenario FS, FILTERW parameter, which represents the width of grass strips along the contours, is modified into 1 m width in the SWAT management database based on preceding studies in Ethiopia (Demissie et al. 2013; Betrie et al. 2011; Hurni 1985).

The second scenario characterizes implementations of SSB (Scenario SSB) on cultivated lands for reducing the rate of sediment yield in the watershed. Stone/soil bunds (SSB) are elevated physical soil and water conservation structures that are constructed along contours on erosion vulnerable land uses (Lemma et al. 2019). Stone/soil bunds (SSB) reduce the volume and speed of overland flow. In addition, it reduces sheet erosion and increase the retention service.

Table 4 Descriptions of the considered BMPs and the parameter changes in the SWAT model database based on the suggestions of literatures (Lemma et al. 2019; Gathagu et al. 2018; Betrie et al. 2011; Waidler et al. 2011; Asres and Awulachew 2010)

Scenario	Description	Adjusted parameter value		
		Parameter	Calibrated	Modified
Baseline	This is the existing conditions in the watershed	*	*	*
Filter strips (FS)	1 m wide grass strips established on cultivated lands	FILTERW	0 (m)	1 (m)
Stone/soil bunds (SSB)	Stone/soil bunds are elevated physical soil and water conservation structures that are constructed along contours on erosion vulnerable land uses	SL_SUBBSN	a	a × 0.50
		HRU_SLP	a	a × 0.75
		CN2	78	59
		USLE_P	0.68	0.32
Grassed waterways (GW)	Runoff in all cultivated lands is removed through grassed waterways	GWATN	a	0.1
		GWATW	a	2.5 m
		GWATD	a	0.3 m
		GWATSPCON	a	0.005
		GWATL	a	b
		GWATS	a	HRU_SLP * 0.75
Reforestation of croplands (RC)	Cultivated lands that are located in slopes higher than 15% are changed into planation forest	Land use change	*	RC and *
FS & RC	Combining filter strips and reforestation of croplands higher than 15% slope	FILTERW and land use change	0 m FILTERW and *	1 m FILTERW, RC and *
GW & RC	Joining grassed waterways and reforestation of croplands that are located above 15% slope	GW parameters and land use change	GW parameters initial values and *	Modified GW parameters values, RC and *
SSB & GW	Implementing stone/soil bunds and grassed waterways together	SSB and GW parameters	SSB, GW and *	Modified SSB and GW parameters values, and *

Note that "*" represents the calibrated flow and sediment parameters values; "a" is the SWAT assigned values; "b" indicates that the grassed waterways length was given based on the length of the HRUs

Soil physicochemical properties which are vital for increasing crop yield are also improved through the implementations of SSB. In addition, SSB reduce gully head developments. In general, SSB increases formation of depositional landforms and limits developments of erosional landscape process such as rill and gully erosion. In the Ethiopian highlands, large efforts have been made to construct SSB in the last five decades which were supported by the government, multilateral agencies, and local and international Non-Governmental Organizations (NGOs) (Gashaw 2015). Consequently, evaluating effectiveness of this soil and water management practice in Gumara watershed is imperative. Hence, the SSB Scenario was implemented in the cultivated lands by changing the curve number (CN2) into 59 and USLE_P into 0.32 (Nyssen et al. 2007a; Betrie et al. 2011). In addition, implementation of SSB is expected to reduce slope length (SL_SUBBSN) by 50% and slope steepness (HRU_SLP) by 25% (Lemma et al. 2019) (Table 4). Consistent with the three slope thresholds given to define HRUs (i.e., 0–5, 5–15 and >15%), SWAT identified three SL_SUBBSN and HRU_SLP values. Thus, the modified SL_SUBBSN and HRU_SLP values were assigned by reducing 50% and 25% for each slope class, respectively.

The third type of BMP considered in this study was GW, which describes water channels where grasses are established along drainage pathways (Gathagu et al. 2018; Waidler et al. 2011). A grassed waterway increases sediment trapping and hence, it enhances deposition of sediment along the channels. It also diminishes peak flow rate velocity in the channel by snowballing hydraulic roughness of flow in the channel. Furthermore, GW reduce gully erosion in the channel fragment by establishing channel cover in stream banks (Arabi et al. 2008). Thus, implementations of GW enhance establishment of depositional landscape process and reduce formation of valleys. Though this type of BMP is less applied in the Ethiopian highlands, evaluating its effectiveness in reducing sediment yield is important for future use. Implementation of the GW scenario in this study was made by altering scheduled management option parameters (MGT_OP 7). In addition, it was applied through changing the Manning's roughness factor "n" (GWATn) for the main channel, channel width (GWATW), channel depth (GWATD), linear parameter for determining sediments

Table 5 Sensitive streamflow and sediment parameters, their rank and fitted values used for flow and sediment simulation

Flow/sediment	Parameter	t-Stat	*P* value	Rank of sensitivity	Fitted value
Streamflow	ALPHA_BF.gw	8.27	0.00	1	0.158
	CN2.mgt	7.34	0.00	2	−0.087
	CH_N2.rte	−2.46	0.01	3	0.092
	CH_K2.rte	−1.96	0.05	4	129
	GWQMN.gw	−1.77	0.08	5	1193
	GW_REVAP.gw	−0.73	0.47	6	0.103
	GW_DELAY.gw	−0.66	0.51	7	167
	REVAPMN.gw	−0.61	0.54	8	355
Sediment	USLE_P.mgt	−16.61	0.00	1	0.68
	USLE_C{AGRC}.plant.dat	−13.84	0.00	2	0.025
	USLE_C{RNGB}.plant.dat	−2.18	0.03	3	0.323
	SPCON.bsn	2.18	0.03	4	0.006
	CH_COV1.rte	2.01	0.04	5	0.045
	SPEXP.bsn	−1.79	0.07	6	1.024
	USLE_C{RNGE}.plant.dat	−1.56	0.12	7	0.311
	CH_COV2.rte	−0.62	0.54	8	0.090

AGRC Cultivated land, *FRST* Forest, *RNGE* Grassland, *RNGB* Shrubland

re-entrained in channel sediment routing (GWATSPCON), length (GWATL) and slope (GWATS) of the GW. The study used GWATn value of 0.1 that indicate dense grasses, 2.5 m GWATW, 0.3 m GWATD and 0.005 GWATSPCON (Gathagu et al. 2018; Waidler et al. 2011; Arabi et al. 2008). The GWATL values were given considering the length of the HRUs while the GWATS was assigned by multiplying the HRUs slope with 0.75 (Waidler et al. 2011) (Table 4).

The fourth BMP scenario, which is the RC scenario (Scenario RC), was aimed to appraise effects of reforestation on erosion vulnerable croplands on rates of sediment yield (Gashaw et al. 2020). Reforestation of croplands (RC) reduces formation of sheet, rill and gully erosion and hence, prevents progress of erosional land forms in the landscapes. In addition, reforestation can also alter intermittent streams into perennial streams. Furthermore, stream bank degradation is reduced along the developed management zones and hence, reduces stream sediment and turbidity. The consideration of the RC scenario in this study was aimed to control soil erosion through avoiding steep slope cultivation (>15% slope) (Gashaw et al. 2020; Jembere et al. 2017; Berhanu et al. 2013). This scenario assumes that adequate food production will be produced in the remaining slope classes through efficient use of agricultural inputs. The RC scenario was implemented in some parts of the Ethiopian highlands since recently to restore degraded croplands in the form of area closure. However, planting trees on the degraded croplands will help for rejuvenating the area in a short time than using area closure alone, and thus, evaluating its effectiveness on soil erosion reduction is essential. The RC scenario was applied by modifying the land use, and the associated SWAT model parameters in the database.

As mentioned above, three blended scenarios such as FS & RC, GW & RC and SSB & GW scenarios were also evaluated in addition to the four independent BMPs. The main intention of evaluating the blended BMPs was to assess effectiveness of combinations of BMPs in reducing sediment yield in the study watershed. Summary of the BMPs considered in the study is given in Table 4.

The mean annual sediment yield results obtained from the baseline situation and considered BMPs was categorized into sediment severity classes and hence, the areas covered are compared at the watershed scale. Furthermore, the estimated mean annual sediment yield and the sediment reduction efficiency of each BMP related to the baseline condition were assessed at the watershed and sub watershed scales. ArcGIS 10.3.1 was used for analysis and mapping purposes.

Results

Sensitive Flow and Sediment Parameters

Sensitivity analysis was made using t-Stat and *P* value. The result shows that among the ten streamflow parameters considered for sensitivity analysis (Table 2), eight of them were found sensitive, which control the output variable (Table 5). The five top sensitive flow parameters from high to low sensitivity were ALPHA_BF, CN2, CH_N2, CH_K2, and GWQMN. The remaining sensitive flow parameters from high to less sensitivity were GW_REVAP, GW_DELAY, and REVAPMN.

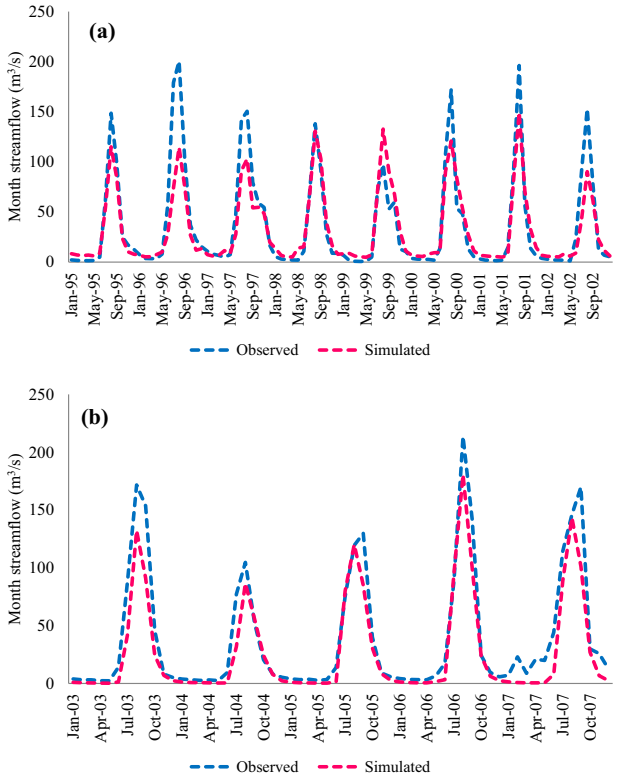

Fig. 5 The monthly streamflow hydrograph in the calibration (**a**) and validation (**b**) periods

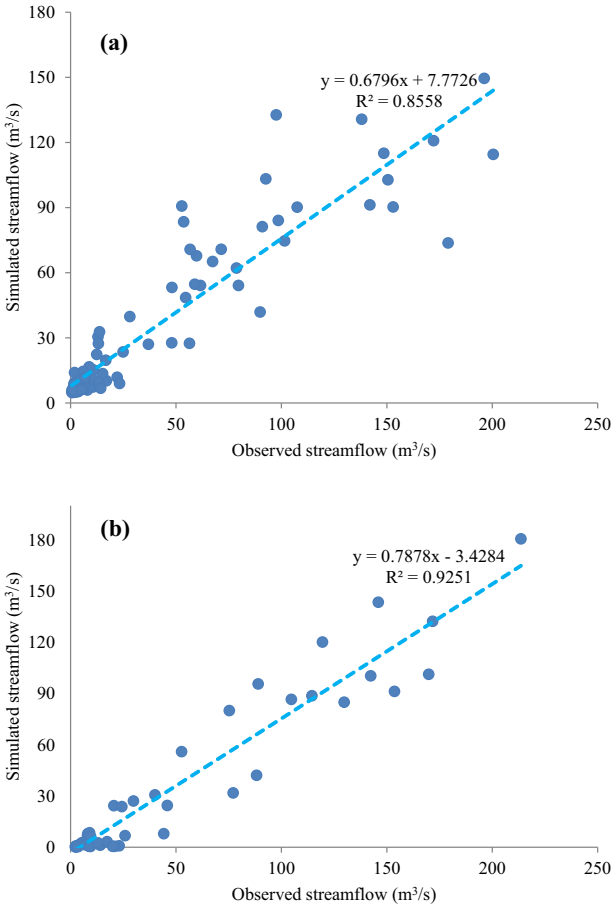

Fig. 6 Scatter plot of the observed and simulated monthly streamflow in the calibration (**a**) and validation (**b**) periods

On the other hand, among the nine sediment parameters where sensitivity analysis was employed (Table 2), eight of them were sensitive to sediment output (Table 5). Of these, the five uppermost sensitive sediment parameters in the order of their sensitivity were USLE_P, USLE_C {AGRC}, USLE_C {RNGB}, SPCON, and CH_COV1. The remaining three sediment sensitive parameters were SPEXP, USLE_C {RNGE} and CH_COV2.

Calibration and Validation Results

The graphical comparisons of observed and simulated streamflow shows that the model has captured observed low and high flows very well in the calibration and validation periods (Fig. 5). Scatter plots that illustrate consistency of observed and simulated flows during the calibration and validation periods (Fig. 6) also demonstrate the good simulation of the model in the watershed. In terms of model performance statistics (Table 6), NSE of 0.81 and 0.86, PBAIS of 10.7 and 13.5% and RSR of 0.43 and 0.38 were achieved at calibration and validation periods, respectively. The obtained R^2 values during the two simulation periods were also higher than 0.75 (Table 5).

In relation to sediment, both the hydrograph (Fig. 7) and the scatter plot (Fig. 8) of observed and simulated sediment illustrate the acceptable simulation of the SWAT model during the two simulation periods. In terms of performance measures, NSE of 0.67 and 0.69, PBAIS of −6.1 and −11.2% and RSR of 0.57 and 0.56 were attained during the calibration and validation periods, respectively (Table 6). The acquired R^2 values were 0.68 in calibration and 0.70 in validation periods (Table 6).

Table 6 Model performance statistics of streamflow and sediment during calibration (1995–2002) and validation (2003–2007) periods

Simulated element	Simulation period	Model performance statistics			
		NSE	PBIAS (%)	RSR	R^2
Streamflow	Calibration	0.81	+10.7	0.43	0.86
	Validation	0.86	+13.5	0.38	0.93
Sediment	Calibration	0.67	− 6.1	0.57	0.68
	Validation	0.69	−11.2	0.56	0.70

Effects of BMPs on Sediment Yield at the Watershed Scale

The mean annual sediment yield of 13 years (1995–2007) was evaluated at the watershed scale at the baseline and

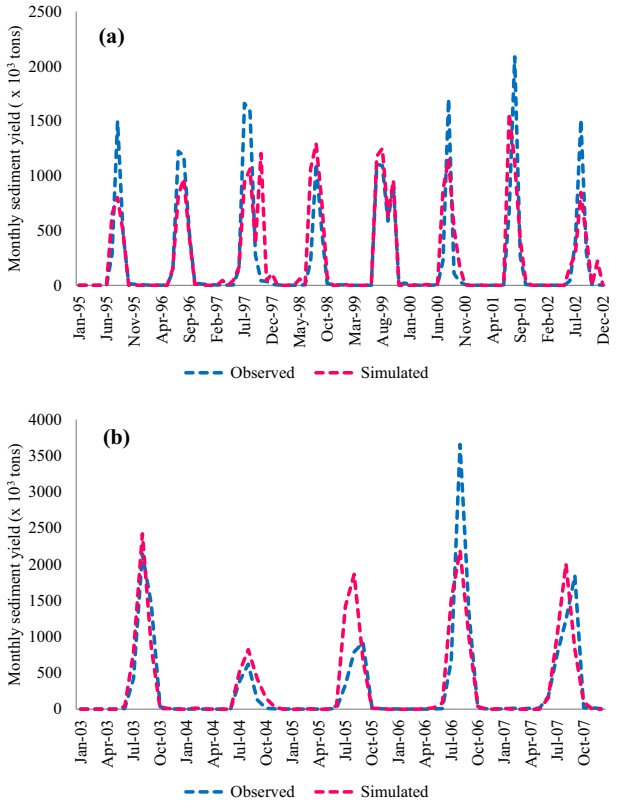

Fig. 7 The monthly sediment yield hydrography of Gumara watershed during the calibration (**a**) and validation (**b**) periods

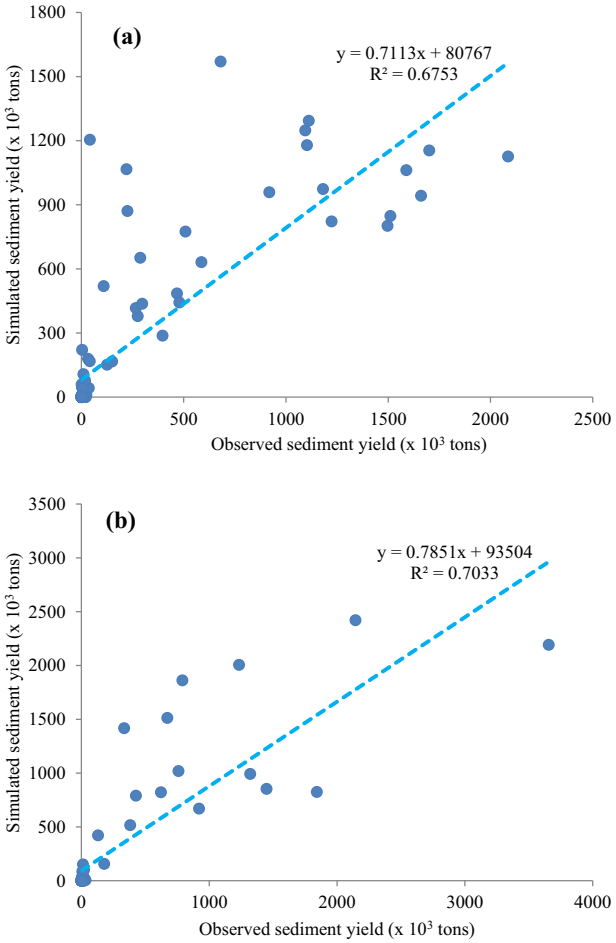

Fig. 8 Scatter plot showing the monthly observed and simulated sediment yield during the calibration (**a**) and validation (**b**) periods

seven plausible BMP scenarios. The obtained sediment yield was categorized into five classes such as 0–5 t ha^{-1} yr^{-1} (very low), 5–11 t ha^{-1} yr^{-1} (low), 11–18 t ha^{-1} yr^{-1} (moderate), 18–25 t ha^{-1} yr^{-1} (high) and 25–38 t ha^{-1} yr^{-1} (very high) (Table 7), which was adapted from previous studies carried out in the Ethiopian highlands (Gashaw et al. 2019; Tamene et al. 2017).

The result revealed that areas covered by the very high erosion sediment severity class reduced in all BMPs (Table 7). For example, at the baseline condition, the very high sediment intensity group accounted about 22.5% of the watershed. However, it reduced into 15.1% at FS Scenario and 7.9% to all the remaining BMPs. The areas covered by the high sediment intensity category have also reduced in all BMPs from the baseline conditions except at the GW Scenario (Table 7). A similar diminished of areas represented by the moderate intensity categories were also taken place. In contrast, the areas represented by the low sediment intensity class have increased in all BMPs compared to the baseline situation. Similarly, the areas covered by the very low sediment intensity class have also increased due to the implementations of SSB, FS & RC, GW & RC, SSB & GW, and GW Scenarios while the application of FS and RC Scenarios did not change areas covered by this sediment intensity category (Table 7). In general, the extents covered by the very high, high and moderate sediment severity classes were reduced in all BMPs (except the high sediment intensity category at the GW Scenario) compared to the present conditions. In contrast, the implementations of the considered BMPs have increased the areas represented by the low and very low sediment intensity categories (except the FS and RC Scenarios at the very low sediment intensity class) (Table 7), demonstrating the evaluated BMPs have reduced sediment yield in the watershed study.

In terms of exposure to assess the areas covered by the very high, high and moderate sediment intensity classes collectively and the low and very low classes together, the areas represented by very high to moderate intensity classes at the baseline condition accounted about 99.7% of the watershed while the remaining 0.3% is accounted by the low and very low classes (Table 7). At the implementations of the FS, SSB, GW and RC Scenarios, the very high, high and moderate sediment severity categories represented 69, 51.1, 81.5 and 58.9% of the study area, respectively. In contrast, the low and very low intensity groups together represented 31% in FS Scenario, 48.9% in SSB Scenario,

Table 7 Percentage of sediment severity classes (Adapted from Gashaw et al. 2019 and Tamene et al. 2017) in a given scenario

SY (t ha^{-1} yr^{-1})	Severity classes	BMB scenarios (area in %)							
		Baseline	FS	SSB	GW	RC	FS & RC	GW & RC	SSB & GW
0–5	Very low	0.0	0.0	4.8	0.3	0.0	4.5	4.8	9.1
5–11	Low	0.3	31.0	44.1	18.2	41.1	44.3	44.0	39.7
11–18	Moderate	42.1	23.6	27.3	34.8	35.0	27.4	27.4	27.4
18–25	High	35.1	30.3	15.9	38.8	16.0	15.9	15.9	15.9
25–38	Very high	22.5	15.1	7.9	7.9	7.9	7.9	7.9	7.9

18.5% in GW Scenario and 41.1% in the RC Scenario (Table 7). Hence, compared to the FS, GW and RC Scenarios, the very high, high and moderate sediment severity categories collectively represented the lowest coverage at the SSB Scenario. Conversely, the low and very low classes together covered the largest areas at the SSB Scenario, indicating that this BMP has the highest sediment reduction efficiency. The second BMP that is efficient for sediment reduction is the RC Scenario. The third and fourth ranked individual effective BMPs are the FS and the GW Scenarios, respectively. Of the considered combined BMPs such as FS & RC, GW & RC, and SSB & GW, the very high, high and moderate sediment intensity classes collectively (51.2%) and the very low and low intensities together (48.8%) represented analogous areas coverage (Table 7). However, at the SSB & GW Scenario, the very low intensity represented greater areas, signifying that this BMP is better than the GW & RC and FS & RC Scenarios in terms of sediment yield reduction at the watershed scale (Table 7).

The long term mean annual sediment yield (1995–2007) of the study watershed at the baseline situations and the considered BMPs, and the reduction efficiency of each scenario against the baseline settings are presented in Fig. 9a and b. The result designated that the mean annual sediment yield at the baseline circumstances is estimated at 19.7 t ha^{-1} yr^{-1} (Fig. 9a). The sediment yield appraised due to implementations of FS, SSB, GW and RC Scenario has provided the mean annual sediment yield of the watershed into 17 t ha^{-1} yr^{-1}, 13.7 t ha^{-1} yr^{-1}, 16.5 t ha^{-1} yr^{-1} and 14.6 t ha^{-1} yr^{-1}, respectively. Consequently, sediment yield has reduced by 13.7% at the FS Scenario, 30.5% by SSB Scenario, 16.2% by GW Scenario and 25.9% by RC Scenario. Hence, from the individual BMPs, the reduction efficiency of the SSB Scenario is very high followed by the RC Scenario. Compared to the individual BMPs, the mean annual sediment yield of the blended BMPs and their reduction efficiency is greater. Of the combined BMPs, the highest reduction efficiency (34%) was achieved through the implementations of the SSB & GW Scenario while the applications of the GW & RC and FS & RC Scenarios reduced the baseline sediment yield by 32% and 29.9%, respectively (Fig. 9b). The FS & RC Scenario showed lesser efficiency than the SSB Scenario.

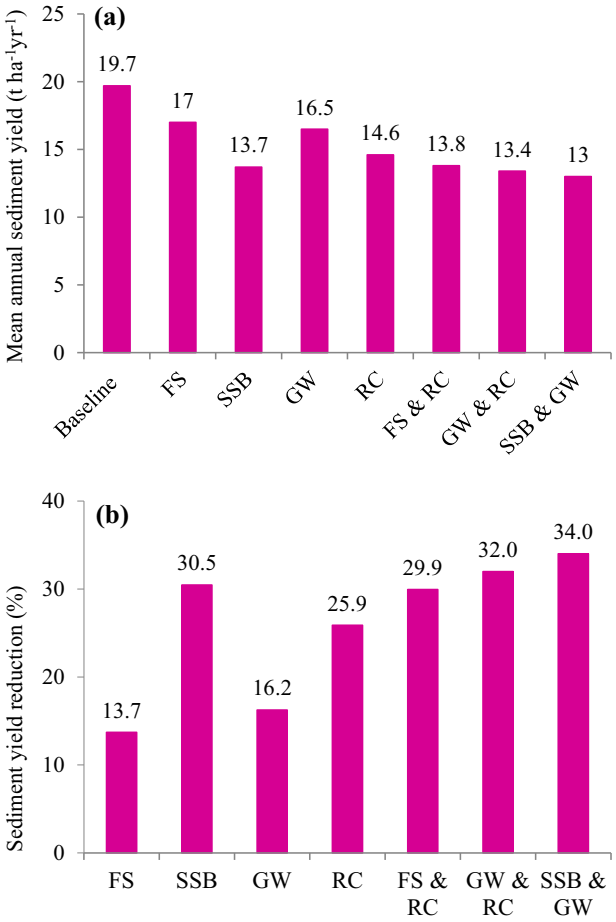

Fig. 9 Mean annual sediment yield at different BMPs (**a**) and sediment yield reductions (%) compared to the baseline scenario at the watershed scale (**b**)

Effects of BMPs on Sediment Yield at the Sub-watershed Scale

The mean annual sediment yield estimated at the baseline situation and the seven considered BMPs at the sub watershed scale are presented in Fig. 10 while the sediment yield reduction efficiency of each BMP against the baseline condition is given in Fig. 11. The findings revealed that at the baseline condition, the mean annual sediment yield ranges from 5 to 38 t ha^{-1} yr^{-1}, indicating that there are no areas under the very low sediment yield intensity class.

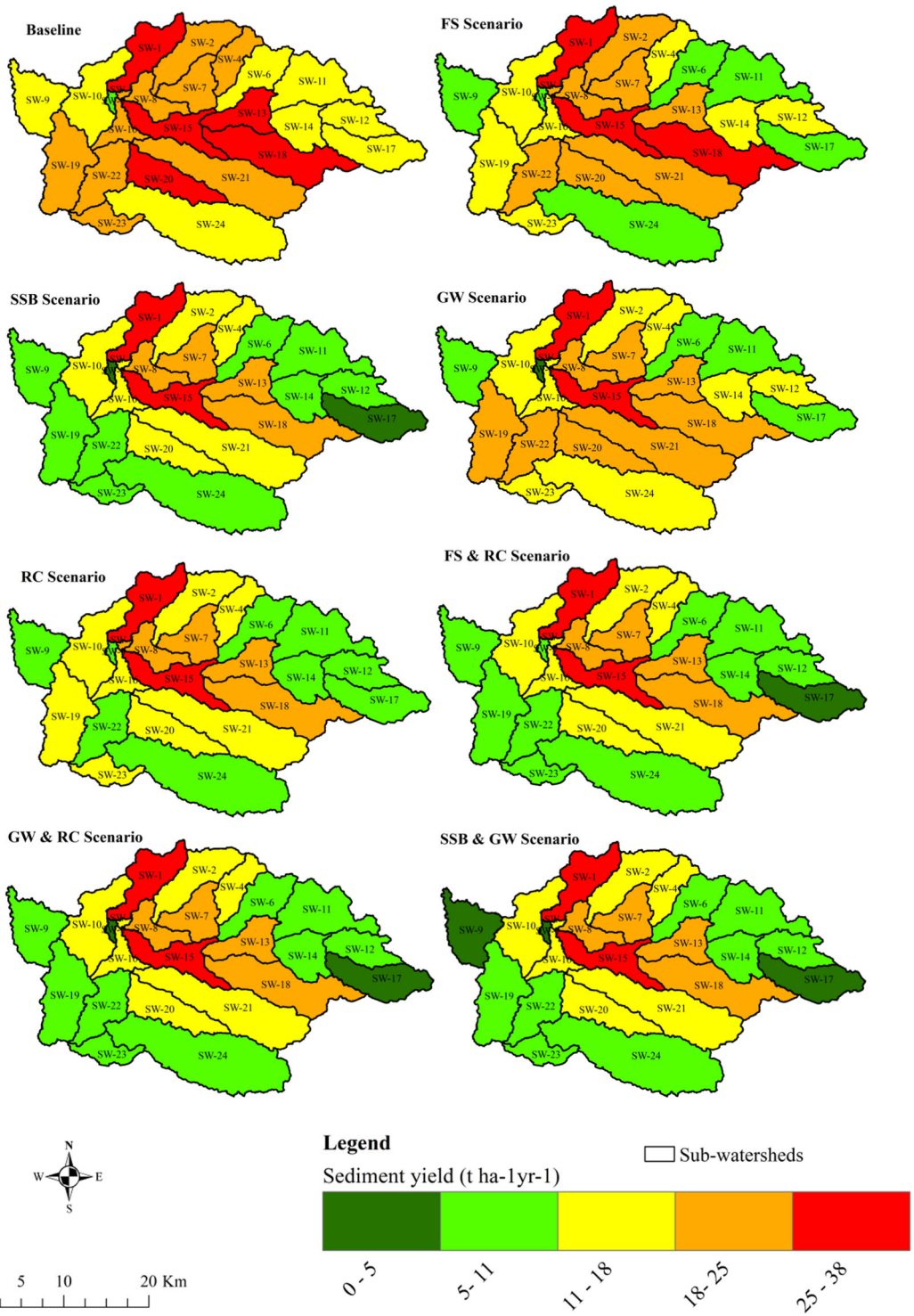

Fig. 10 Mean annual sediment yield (1995–2007) at the sub watershed scale under the baseline conditions, FS Scenario, SSB Scenario, GW Scenario, RC Scenario, FS & RC Scenario, GW & RC Scenario and SSB & GW Scenario

At baseline conditions, SW-1, SW-13, SW-15, SW-18 and SW-20 are undergoing very high sediment intensity, which ranges from 25 to 38 t ha^{-1} yr^{-1}. In addition, there are ten sub watersheds under the high sediment severity category (i.e., SW-2, SW-4, SW-5, SW-7, SW-8, SW-16, SW-19, SW-21, SW-22 and SW-23). Areas experiencing high to very high sediment severity categories are attributed mainly to slope and percent of cultivated land and grassland.

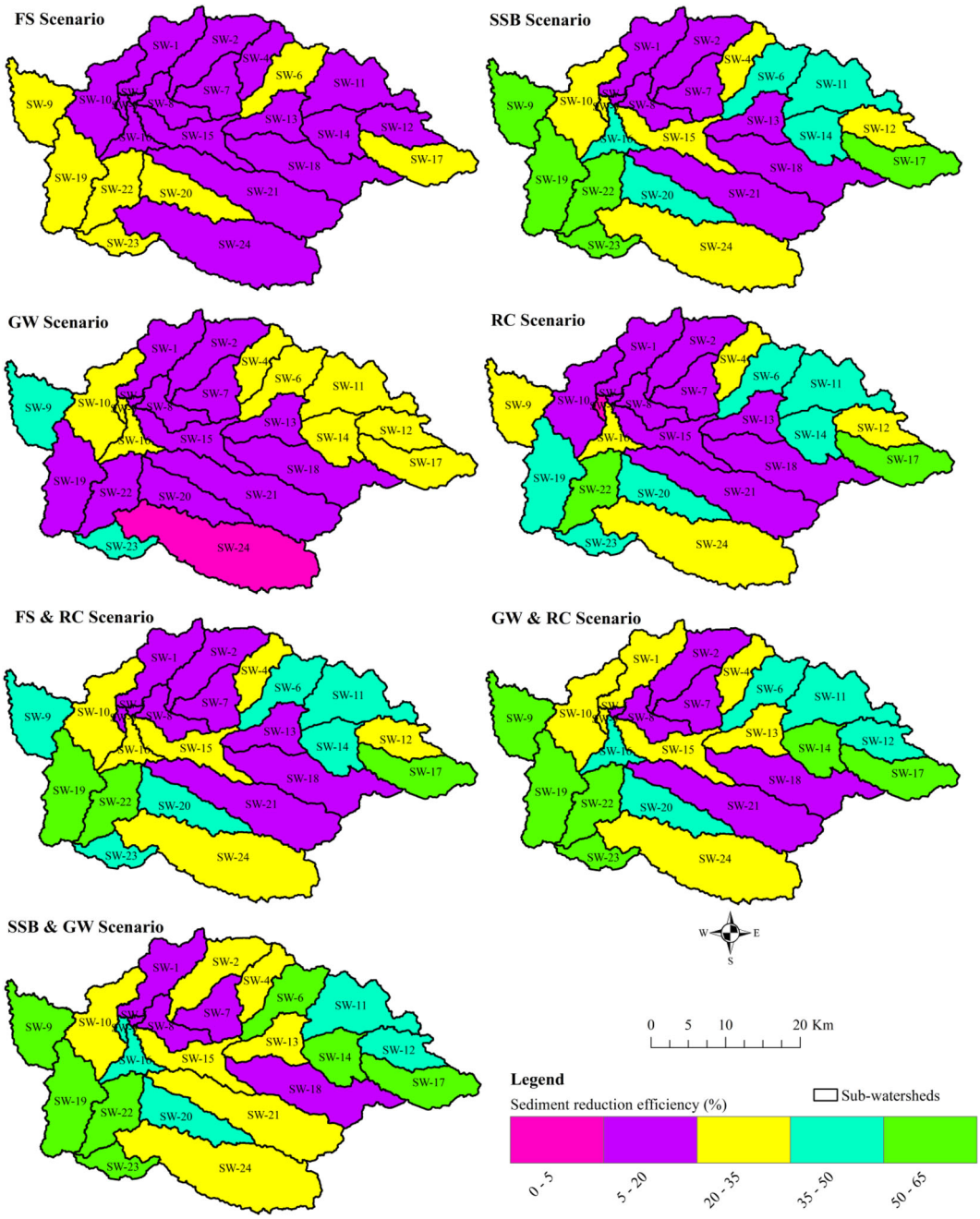

Fig. 11 Sediment reduction efficiency (%) at each sub-watershed after implementation of FS Scenario, SSB Scenario, GW Scenario, RC Scenario, FS & RC Scenario, GW & RC Scenario and SSB & GW Scenario

In those sediment severity classes, about 70–96% of the sub watersheds are covered by slope classes of 5–15 and >15%, where majority of areas in nearly 80% of the sub watersheds are represented by slopes higher than 15%. While cultivated land and grassland together in these sediment severity classes represent about 78–97% of the sub watersheds, of which cultivated land in above 73% of the sub watersheds represent above 65%. The sub watersheds suffering the moderate intensity class is SW-6, SW-9, SW-10, SW-11, SW-12, SW-14, SW-17 and SW-24. On the other hand, SW-3 is within the low sediment intensity category.

The mean annual sediment yield due to implementations of FS Scenario is similar with the baseline conditions, which ranges from 5 to 38 t ha^{-1} yr^{-1}. However, at the FS Scenario, only SW-1, SW-15 and SW-18 are within the very high sediment intensity category, and SW-13 and SW-20 were shifted down to the high sediment intensity cluster. In addition, the FS Scenario has also shifted areas

Table 8 Suggested BMPs for moderate to very high sediment producing sub watersheds (i.e., >11 t ha yr^{-1} SY) and priority ranks of sub-watersheds for implementations of the suggested BMPs

Sub-watersheds	Suggested BMPs in sequential order	Priority ranks for implementations of suggested BMPs
SW-1	GW & RC, GW & SSB, FS & RC, and SSB	1
SW-2	SSB & GW, GW & RC, SSB, and FS & RC	13
SW-4	SSB & GW, GW & RC, FS & RC, and SSB	14
SW-5	SSB & GW, GW & RC, GW, and SSB	12
SW-6	SSB & GW, GW & RC, SSB, and FS & RC	22
SW-7	SSB & GW, GW & RC, SSB, and FS & RC	8
SW-8	SSB & GW, GW & RC, GW, and SSB	7
SW-9	SSB & GW, GW & RC, SSB, and GW	19
SW-10	SSB & GW, GW & RC, SSB, and FS & RC	16
SW-11	SSB & GW, GW & RC, SSB, and FS & RC	21
SW-12	SSB & GW, GW & RC, SSB, and FS & RC	18
SW-13	SSB & GW, GW & RC, FS & RC, and SSB	4
SW-14	GW & RC, SSB & GW, FS & RC, and RC	17
SW-15	SSB & GW, GW & RC, FS & RC, and SSB	2
SW-16	SSB & GW, GW & RC, SSB, and FS & RC	15
SW-17	SSB & GW, GW & RC, FS & RC, and SSB	23
SW-18	GW & RC, SSB & GW, FS & RC, and SSB	3
SW-19	SSB & GW, SSB, FS & RC, and GW & RC	9
SW-20	SSB & GW, GW & RC, SSB, and FS & RC	5
SW-21	SSB & GW, SSB, GW & RC, and FS & RC	11
SW-22	GW & RC, FS & RC, SSB & GW, and SSB	6
SW-23	SSB & GW, GW & RC, SSB, and FS & RC	10
SW-24	SSB & GW, SSB, FS & RC, and GW & RC	20

undergoing the high intensity class to the moderate sediment category. Conversely, the areas under the low sediment intensity categories are improved after the implementation of the FS Scenario, which were basically moved from the moderate intensity class (Fig. 10). In terms of assessing the sediment reduction efficiency, sediment yield with the implementation of the FS Scenario has reduced from 5 to 35%, and in the preponderance areas of the watershed, this Scenario reduced sediment from 5 to 20% (Fig. 11).

At the implementation of the SSB Scenario, the mean annual sediment yield of the considered watershed ranges from 0 to 38 t $ha^{-1}yr^{-1}$. In the application of the SSB Scenario, only SW-1 and SW-15 are persisting under the very high sediment intensity class while SW-13 and SW-18 were moved down to the high intensity group. In addition, SW-20 was shifted into the moderate sediment intensity category (Fig. 10). The SSB Scenario has also shifted areas experiencing the high sediment intensity class into the moderate category, and the moderate category into the low and very low categories (Fig. 10). For example, SW-17 was facing the moderate sediment intensity class, but the SSB Scenario has shifted this sub watershed into the very low sediment intensity category. In terms of looking its efficiency for reducing sediment yield, the SSB Scenario has condensed sediment yield from 5 to 65% (Fig. 11). The highest sediment yield reduction efficiency (i.e., 50–65%) at the implementations of this BMP is detected in SW-9, SW-17, SW-19, SW-22 and SW-23 (Fig. 11).

The mean annual sediment yield of the watershed under the GW Scenario ranges from 0 to 38 t $ha^{-1}yr^{-1}$(Fig. 10). The application of this BMP has moved areas suffering the very high sediment intensity cluster into the high sediment intensity set (i.e., SW-13, SW-18 and SW-20) (Fig. 10). The sub watersheds where the implementation of the GW Scenario did not changed compared to the baseline conditions is SW-1 and SW-15 from the very high sediment intensity, SW-7, SW-8, SW-19, SW-21 and SW-22 from the high sediment intensity class and SW-12, SW-14, SW-24 and SW-10 from the moderate intensity category (Fig. 10). The implementation of the GW Scenario has bargain sediment yield from 0 to 50%, but in the majority of the sub watersheds, it reduced sediment from 5 to 20%. The sediment reduction efficiency of the GW Scenario is very efficient (i.e., 35–50%) in SW-9 and SW-23 (Fig. 11).

The RC Scenario has moved areas from the very high and high sediment intensity categories into the moderate sediment severity assemblage. Besides, the high, moderate

and low sediment intensity categories have also moved into the lower sediment intensity sets at the implementations of the RC Scenario. The mean annual sediment yield of the study area within the RC Scenario is from 5 to 38 t $ha^{-1}yr^{-1}$ (Fig. 10). The RC Scenario did not shift SW-1 and SW-15 from the very high sediment intensity category. Moreover, this Scenario has not changed SW-7 and SW-8 from the high intensity class and SW-10 from the moderate sediment category. In terms of its efficiency, the application of the RC Scenario reduced sediment yield from 0 to 65%. The RC Scenario is more efficient for SW-17 and SW-22, where the sediment is reduced from 50 to 65% (Fig. 11).

The implementations of the combined BMPs such as FS & RC, GW & RC, and SSB & GW Scenarios have also reduced the SW-13, SW-18 and SW-20 from the very high sediment intensity category and these sub watersheds were shifted into the high and moderate severity classes (Fig. 10). In addition, the three blended Scenarios have also resulted in the shift from the highest sediment intensity classes into the lower sediment categories. However, the applications of any of the combined Scenarios did not change the SW-1 and SW-15 into the less sediment severity categories. The annual sediment yield of these Scenarios is almost identical except in two sub watersheds (i.e., SW-9 and SW-3) (Fig. 10). However, the reduction efficiency of the three blended BMPs is slight different. Comparatively, SSB & GW is more efficient followed by the GW & RC Scenario at the sub watershed scale (Fig. 11).

In general, from the individual BMPs, the reduction efficiency achieved under the application of the SSB Scenario is very high in the greatest sub watersheds (Fig. 11). The second, third, and fourth ranged effective BMPs at the sub watershed scales are the RC, GW and FS Scenarios, respectively. Of the combined BMPs, as it is mentioned above, the SSB & GW Scenario has the highest efficiency followed by the GW & RC Scenario in most sub watersheds. However, the GW & RC performed better than the SSB & GW Scenario in particular sub watersheds (Fig. 11). In relation to the sediment reduction efficacy of the SSB, and FS & RC Scenarios, they have different performance in the sub watersheds. For some sub watersheds, the SSB reduced better sediment yield while in some others, the FS & RC Scenario has greater sediment reduction efficiency (Fig. 11). Hence, the study disclosed that the implantations of the combined Scenarios mainly SSB & GW and GW & RC Scenarios can reduced the ongoing sediment rate in the study watershed. However, in cases where applying the combined Scenarios is not possible, the SSB Scenario can reduce the significant sediment yield losses in the watershed study.

Though the SSB & GW, GW & RC, SSB, FS & RC, and GW Scenarios are general good in terms of sediment yield reduction in this watershed (Table 8), the effectiveness of each BMP is different within the sub watersheds. Hence, subsequent arrangement of the BMPs based on their efficiency is important to reduce sediment yield at the most. Accordingly, suggestion of the five subsequent efficient BMPs is provided for the critical sediment producing sub watersheds (Table 8). Implementing the first suggested BMP for each watershed (i.e., GW & RC Scenario in SW-1, SW-14, SW-18 and SW-22, and the SSB & GW Scenario in the remaining sub watersheds) (Table 8) provides a mean annual sediment yield of 12.8 t $ha^{-1}yr^{-1}$ at the watershed scale, which reduced the baseline sediment yield by 35%. In addition, application of the above mentioned optimum BMPs would reduce sediment yield from 13.9 to 70% at the sub watershed scale. Since applying BMPs practices in all the critical sediment producing sub watersheds (i.e., >11 t $ha^{-1}yr^{-1}$) is not possible at the same time due to economy and time limitations, prioritization of sub watersheds for implementations of the identified BMPs is imperative (Gashaw et al. 2017; Welde 2016; Bewket and Teferi 2009). For example, because of the high sediment yield identified in SW-1, the leading priority for implementation of the suggested BMPs is given to it. While, the second, third, fourth and fifth prioritization should be given to SW-15, SW-18, SW-13 and SW-20, respectively (Table 8).

Discussions

Calibration and Validation Results

The obtained NSE (>0.75), RSR (<0.50) and R^2 (>0.75) values during the streamflow calibration and validation phases indicates that the SWAT model has very good performance in predicting streamflow while the PBAIS (<15%) signifies its good performance (Moriasi et al. 2007; Begou et al. 2016). On the other hand, the acquired NSE (0.67 and 0.69), R^2 (0.68 and 0.70) and RSR (0.57 and 0.56) values during the sediment calibration and validation time respectively revealed the model's good performance in simulating observed sediment (Moriasi et al. 2007). On the other hand, the performance of SWAT in terms of PBIAS (i.e., −6.1% in calibration and −11.2% in validation periods) is rated as very good (Table 6).

In general, the performance of SWAT model (if NSE, RSR and R^2 are accounted) during the validation periods of streamflow and sediment are better than the calibration phases, which depicts the good quality of the entire streamflow and sediment data. Previous studies in Ethiopia such as in Andassa watershed (Gashaw et al. 2018) and Gilgel Abay catchment (Uhlenbrook et al. 2010) and elsewhere in upper San Pedro watershed, Mexico (Nie et al. 2011) have also obtained a higher model performance efficiency during the validation period compared to their

calibration periods. On the other hand, the performance of SWAT (i.e., considering NSE, RSR and R^2) in simulating streamflow in the present study is better than sediment, which is reasonable as there are complexities of factors affecting sediment dynamics and hence, the model did not easily represent all of those factors. However, in terms of PBIAS, the sediment simulation is better than streamflow.

Effects of BMPs on Sediment Yield at the Watershed and Sub Watershed Scales

In the present study, about 99.7% of the study areas are estimated as erosion vulnerable areas (>11 t ha^{-1} yr^{-1}). However, earlier study in the same watershed reported that nearly 72% of the Gumara watershed was erosion prone, which is contributing to a mean annual sediment yield from 11 to 22 t ha^{-1}yr^{-1} (Asres and Awulachew 2010). The difference in extent of erosion vulnerable area by this study and Asres and Awulachew (2010) is attributable to the low plains of the watershed (ungagged) are included in the previous study, which probably reduced the estimated sediment yield. However, the mean simulated sediment yield at the baseline condition in the present study (i.e., 19.7 t ha^{-1} yr^{-1}) is very much close with Asres and Awulachew (2010) report at both the calibration (18.6 t ha^{-1} yr^{-1} during 1998–2002) and validation (19.2 t ha^{-1} yr^{-1} during 2003–2005) phases. The obtained mean sediment yield from this study is also related to other studies undertaken in the highland parts of the country such as Gashaw et al. (2019) in Andassa watershed (20.3 t ha^{-1} yr^{-1}), Setegn et al. (2010) in the Anjeni-gauged watershed (i.e., 24.6 t ha^{-1} yr^{-1}) and Tamene et al. (2017) in Laelaywukro catchment (i.e., 20 t ha^{-1} yr^{-1}).

The very high and high sediment severity categories (i.e., sediment yield >18 t ha^{-1} yr^{-1}) attributed mainly to steep slope and higher percent of cultivated land and grassland in this study is aligned to preceding findings in the highlands parts of Ethiopia. For example, the high to very high soil erosion severity classes (>80 t ha^{-1} yr^{-1}) in Chemoga watershed are mainly located in steep slopes where the land is cultivated or overgrazed (Bewket and Teferi 2009). In addition, Lemma et al. (2019) in Lake Tana sub basin, where the study area is part of it, also reported that the distinguishing feature of erosion hotspot areas are mainly linked to slope (70% of the sub watersheds has slope > 15%), percentage of cultivated land (>80%) and rainfall (>1000 mm). The uppermost soil erosion rates in Geleda watershed were also observed in the steeper slope areas (i.e., slopes >30%) and where the land is cultivated (Gashaw et al. 2017). Likewise, the steep slopes areas of the Andassa watershed are prone to the extraordinary soil loss rates (i.e., >50 t ha^{-1} yr^{-1}) (Gashaw et al. 2019). Demissie et al. (2013) in Gilgel Gibe Basin has also indicated that high rate of soil erosion were found in sub basins where dry land cropland and pasture covered a maximum percentage of nearly 60%.

The highest sediment yield reductions achieved under the SSB Scenario in the present study is consistent with the findings of previous studies in the highlands of Ethiopia. For example, SSB have reduced soil loss by 25–38% in experimental plots of Gumara-Maksegnit watersheds (Melaku et al. 2018). A study undertaken on several plots of Tigray highlands (northern Ethiopia) also indicated that stone bunds on different ages (3–21 years) reduced sheet and rill erosion by 68%, and increased grain yield and infiltration (Nyssen et al. 2007a). Nyssen et al. (2007b) also revealed that exclosures and stone bunds trapped nearly 74% of the total soil loss in May Zegzeg catchment (northern Ethiopia). Ebabu et al. (2019) study in 42 runoff plots of the Upper Blue Nile Basin also indicated that soil bund reinforced with grass in croplands is one of the most effective management practices for lessening runoff and soil loss. Likewise, Betrie et al. (2011) in the Upper Blue Nile Basin and Lemma et al. (2019) in Lake Tana sub basin indicated that SSB reduced sediment yield by 9–69%, and 61%, respectively. In addition, SWAT based implementation of SSB in Gilgel Gibe Basin has condensed sediment yield by 81% (Demissie et al. 2013).

The effectiveness of the RC Scenario is also reported in several studies undertaken in the Ethiopian highlands, such as Lemma et al. (2019) in Lake Tana sub basin (Ethiopia) and Betrie et al. (2011) in Upper Blue Nile Basin. For example, the implementations of reforesting steep slopes has reduced sediment yield by 61% in Lake Tana sub basin (Lemma et al. 2019) and 46–77% in the Upper Blue Nile Basin (Betrie et al. 2011). The reforestation of steep slope has also reduced the baseline soil erosion rate by 9.1% in the Gilgel Gibe Basin (Demissie et al. 2013), where the reported low reduction efficiency of this BMP was mainly explained by the small area implementations. The effectiveness of GW observed in the study watershed is also consistent with other findings elsewhere. For example, GW for a watershed in southeastern Iowa (USA) has reduced sediment yield by 65% (Dermisis et al. 2010). A considerable sediment yield reduction with the implementation of the GW was also reported in Thika-Chania catchment, Kenya (Gathagu et al. 2018).

The sediment reductions observed at FS Scenario in this study, though its efficiency is lower than the considered independent BMPs, is related with others findings. For example, Asres and Awulachew (2010) in Gumara watershed (same study area) also indicated that the installation of 5 m FS on erosion susceptible land use types reduced sediment yield by 58%. In addition, sediment reductions from 29 to 68% in the Upper Blue Nile Basin (Betrie et al. 2011), 51% in Lake Tana sub basin (Lemma et al. 2019) and 35% in Gilgel Gibe Basin (Demissie et al. 2013) were

reported for 1 m grass contour strips. Mekonnen et al. (2016) study in Debre Mewi watershed (northwest Ethiopia) also indicated the considerable role of ingenious grasses (when used as filter strip) for reducing soil loss from Teff fields (up to 8% slope). Implementations of 2 m FS in El Beal watershed (Southeast Spain) has also reduced sediment yield by 4%, which is extremely very low compared to the sediment reduction efficiency of check dam and reforestations (López-Ballesteros et al. 2019).

Of the considered seven BMPs, the highest sediment yield reduction was achieved in the two blended Scenarios, namely in SSB & GW and GW & RC Scenarios. Similar to this finding, the combinations of structural and vegetative measures was the best way to control soil erosion and its consequences in the runoff plots of the Upper Blue Nile Basin (Ebabu et al. 2019). Bosch et al. (2013) in Lake Erie watersheds (United States) has also reported that the greatest sediment yield reduction was achieved through combinations of BMPs (i.e., cover crop, FS and no-tillage) than the individual BMPs. A study by López-Ballesteros et al. (2019) in El Beal watershed (Southeast Spain) also indicated that implementations of check dam restoration and reforestation independently reduced annual sediment loads by 90% and 27%, respectively at the watershed scale while combination of the two management practices condensed the baseline sediment yield by 92%. In addition, application of GW and terraces in Thika-Chania catchment (Kenya) reduced the baseline sediment yield by 53.9 and 80.7%, respectively while the combined BMPs reduced sediment yield by 88.72% (Gathagu et al. 2018). Furthermore, Uniyal et al. (2020) has also indicated the good performance of the combined BMPs in controlling sediment yield than individual BMPs in the Baitarani watershed (India).

The findings of this study will have broader scientific contributions for similar agro-ecological regions elsewhere in the world in which water-induced soil erosion is a serious challenge for environmental protection and socio-economic developments as well as in areas where continuously monitored sediment data is not available. For example, one of the lessons learned from the present research is that since the effectiveness of each individual and blended BMPs varies within sub watersheds, identifying the most efficient BMP in sub watersheds (>11 t ha^{-1} yr^{-1}) is important to implement successful soil erosion reduction programs. For example, of the considered individual BMPs, the SSB Scenario (30.5%) resulted in the highest soil erosion reduction followed by the RC (25.9%) and GW (16.2%) Scenarios at the watershed scale. However, the GW Scenario showed better sediment reduction efficiency in certain sub watersheds than the SSB and RC Scenarios (Table 8). Similarly, from the blended BMPs, the sediment reduction performance of the SSB & GW Scenario is superior to the GW & RC Scenario at the watershed scale. Nevertheless, GW & RC Scenario showed better sediment reduction efficiencies for specific sub watersheds (Table 8). In addition, evaluating combinations of two or more BMPs was necessary for identifying effective BMPs that provided a high soil loss reduction and thereby lessening its onsite and offsite negative environmental externalities. The concept of evaluating the effectiveness of particular and blended BMPs at the watershed and sub watershed scales can help to identify effective BMPs that can reduce agricultural nutrients and improve water resource availability to ensure sustainable water resources management in times of climate change. The study also developed a method that effectively estimate sediment yield during wet and dry seasons that can be used for impact studies in data-scarce regions.

Limitations of the Study

Since continuous daily and monthly sediment yield data are not available for the study watershed and for that matter in Ethiopia, the study established sediment rating curves for the wet and dry seasons to predict sediment yield at daily bases, which were then aggregated into monthly values. Though the approach is a standard approach in many studies globally due to the absence of continuously monitored sediment records (e.g., Beskow et al. 2009; Welde 2016; Aga et al. 2018; Batista et al. 2017; Gashaw et al. 2019) the applied method may introduce some uncertainties in predicting sediment yield. Besides, the study used a static land use data to evaluate impacts of interventions, although land use is a dynamic biophysical factor that changes over time. Furthermore, though the length of streamflow and sediment data are sufficient to calibration and validation of the SWAT model, due to the absence of recently reported data, the study used streamflow and sediment data that were collected from 1995 to 2007 periods. Likewise, previous studies in the watershed (Dile et al. 2016; Worqlul et al. 2018) used similar streamflow data due to an unavailability of recent data. Another limitation of this study is that the economic feasibility of the studied BMPs were not assessed. Despite the limitations, we used the best available data and robust modeling framework to develop a decision support system that assesses the impacts of BMPs on soil erosion.

Conclusions

In this study, four single (i.e., FS, SSB, GW, and RC) and three combined BMP (i.e., FS & RC, GW & RC, and SSB & GW) Scenarios were evaluated for effectiveness to reduce soil erosion using the SWAT model. The result indicated that about 99.7% of the watershed was vulnerable to erosion at the baseline condition, experiencing mean annual sediment yield that ranged 11–38 t ha^{-1} yr^{-1}.

Implementation of the BMPs reduced sediment yields in the severity classes of very high, high and moderate (except the high sediment intensity category at the GW Scenario). In contrast, implementation of the BMPs increased areas represented by low and very low sediment intensity categories (except the GW and RC Scenarios at the very low intensity), suggesting that the BMPs considered reduce sediment yield in the watershed studied. From the individual BMPs, the reduction effectiveness of the SSB Scenario (30.5%) was very high followed by the RC Scenario (25.9%) and GW Scenario (16.2%). In contrast, implementation of the FS Scenario reduced sediment yield by 13.7%. Of the blended BMPs, applications of the SSB & GW, GW & RC and FS & RC Scenarios reduced sediment yield by 34%, 32% and 29.9%, respectively. Thus, the FS & RC Scenario showed relatively lesser effectiveness than the SSB Scenario at catchment scale. Hence, this study concludes that the combined Scenarios of SSB & GW and GW & RC can significantly reduce sediment yield in the watershed. However, in cases where applying the combined Scenarios is not possible, the SSB Scenario is useful to reduce sediment yield considerably. The identified effective BMPs can be implemented in the Ethiopian highlands and other similar agro-ecological regions in the world to reduce soil erosion and its negative externalities. However, further studies are required to assess the holistic impacts of implementing BMPs. For example, assessing the cost-benefits, on and off-site ecological benefits and farmers preference on different BMPs. In addition, it is also imperative to understand the effects of these BMPs on groundwater and evapotranspiration. Further studies are also important on additional technology choices, including bunds stabilized with multipurpose shrubs or grass, stream buffer treatment, gully treatment, etc.

Acknowledgements The Ethiopian National Meteorological Services Agency (NMSA) provided the climate data while the Ministry of Water, Irrigation and Electricity (MoWIE) of Ethiopia have given the streamflow and sediment data. The authors greatly acknowledge these institutions for providing the data. Furthermore, the authors are also very much grateful for the two anonymous reviewers and the Editor for their constructive comments.

Compliance with ethical standards

Conflict of interest The authors declare no competing interests.

Publisher's note Springer Nature remains neutral with regard to jurisdictional claims in published maps and institutional affiliations.

References

Abbaspour K (2014) SWAT-CUP 2012: SWAT Calibration and Uncertainty Programs – A User Manual. p 106.

Aga AO, Chane B, Melesse AM (2018) Soil erosion modelling and risk assessment in data scarce Rift Valley Lake Regions, Ethiopia. Water 10:1684. https://doi.org/10.3390/w10111684

Ahmed AA, Ismail UHAE (2008) Sediment in the Nile River System. UNESCO International Hydrological Programme. International Sediment Initiative. p 93.

Anteneh W, Mengist M, Wondie A, Tewabe D, Kidan W, Assefa A, Engida W (2014) Water hyacinth coverage survey report on Lake Tana, Technical Report Series 1. Bahir Dar University, Ethiopia. p 29.

Arabi M, Frankenberger JR, Engel BA, Arnold JG (2008) Representation of agricultural conservation practices with SWAT. Hydrol Process 22(10):3042–3055

Arnold J, Moriasi D, Gassman P, Abbaspour K, White M, Srinivasan R, Santhi C, Harmel R, van Griensven A, Van Liew M, Kannan N, Jha M (2012) SWAT: Model use, calibration, and validation. Trans ASABE 55(4):1491–1508

Arnold J, Srinivason R, Muttiah R, Williams J (1998) Large area hydrologic modeling and assessment. Part I: model development. J Am Water Resour Assoc 34(1):73–89

Asres MT, Awulachew SB (2010) SWAT based runoff and sediment yield modelling: a case study of the Gumera watershed in the Blue Nile Basin. Ecohydrol Hydrobiol 10(2–4):191–199

Awulachew SB, McCartney M, Steenhuis TS, Ahmed AA (2008) A review of hydrology, sediment and water resource use in the Blue Nile basin. International Water Management Institute, Colombo, Sri Lanka, p 87. IWMI Working Paper 131

Batista PVG, Silva MLN, Silva BPC, Curi N, Bueno IT, Júnior FWA, Davies J, Quinton J (2017) Modelling spatially distributed soil losses and sediment yield in the upper Grande River Basin-Brazil. Catena 157:139–150

Begou J, Jomaa S, Benabdallah S, Bazie P, Afouda A, Rode M (2016) Multi-site validation of the SWAT model on the Bani catchment: model performance and predictive uncertainty. Water 8:178. https://doi.org/10.3390/w8050178

Berhanu B, Melesse AM, Seleshi Y (2013) GIS-based hydrological zones and soil geo-database of Ethiopia. Catena 104:21–31. https://doi.org/10.1016/j.catena.2012.12.007

Beskow S, Mello CR, Norton LD, Curi N, Viola MR, Avanzi JC (2009) Soil erosion prediction in the Grande River basin, Brazil using distributed modeling. Catena 79:49–59

Betrie GD, Mohamed YA, van Griensven A, Srinivasan R (2011) Sediment management modelling in the Blue Nile Basin using SWAT model. Hydrol Earth Syst Sci 15(3):807–818

Bewket W, Teferi E (2009) Assessment of soil erosion hazard and prioritization for treatment at the watershed level: case study in the Chemoga watershed, Blue Nile basin, Ethiopia. Land Degrad Dev 20:609–622

Blanco H, Lal R (2008) Principles of soil conservation and management. Springer Science+Business Media B.V, Berlin, p 240

Bosch NS, Allan JD, Selegean JP, Scavia P (2013) Scenario-testing of agricultural best management practices in Lake Erie watersheds. J Gt Lakes Res 39:429–436

Briak H, Mrabet R, Moussadek R, Aboumaria K (2019) Use of a calibrated SWAT model to evaluate the effects of agricultural BMPs on sediments of the Kalaya river basin (North of Morocco). Int Soil Water Conserv Res 7:176–183

Demissie TA, Saathoff F, Seleshi Y, Gebissa A (2013) Evaluating the Effectiveness of Best Management Practices in Gilgel Gibe Basin Watershed-Ethiopia. J Civ Eng Arch 7(10):1240–1252

Dermisis D, Abaci O, Papanicolaou AN, Wilson CG (2010) Evaluating grassed waterway efficiency in southeastern Iowa using WEPP. Soil Use Manag 26:183–192

Dersseh MG, Kibret AA, Tilahun SA, Worqlul AW, Moges MA, Dagnew DC, Abebe WB, Melesse AM (2019) Potential of Water

Hyacinth Infestation on Lake Tana, Ethiopia: a Prediction Using a GIS-Based Multi-Criteria Technique. Water 11:1921
Dile Y, Daggupati P, George C, Srinivasan R, Arnold J (2016) Introducing a new open source GIS user interface for the SWAT model. Environ Model Softw 85:129–138
Ebabu K, Tsunekawa A, Haregeweyn N, Adgo E, Meshesha DT, Aklog D, Masunaga T, Tsubo M, Sultan D, Fenta AA, Yibeltal M (2019) Effects of land use and sustainable land management practices on runoff and soil loss in the Upper Blue Nile basin, Ethiopia. Sci Total Environ 648:1462–1475
Engebretsen A, Vogt RD, Bechmann M (2019) SWAT model uncertainties and cumulative probability for decreased phosphorus loading by agricultural Best Management Practices. Catena 175:154–166
Gashaw T (2015) The implications of watershed management for reversing land degradation in Ethiopia. Res J Agric Environ Manag 4(1):5–12
Gashaw T, Tulu T, Argaw M (2017) Erosion risk assessment for prioritization of conservation measures in Geleda watershed, Blue Nile Basin, Ethiopia. Environ Syst Res 6:1
Gashaw T, Tulu T, Argaw M, Worqlul AW (2018) Modeling the hydrological impacts of land use/land cover changes in the Andassa watershed, Blue Nile basin, Ethiopia. Sci Total Environ 619-620:1394–1408
Gashaw T, Tulu T, Argaw M, Worqlul AW (2019) Modeling the impacts of land use-land cover changes on soil erosion and sediment yield in the Andassa watershed, Upper Blue Nile Basin, Ethiopia. Environ Earth Sci 78:679
Gashaw T, Worqlul AW, Dile YT, Addisu S, Bantidar A, Zeleke G (2020) Evaluating potential impacts of land management practices on soil erosion in the Gilgel Abay watershed, Upper Blue Nile Basin, Ethiopia. Heliyon 6:e04777
Gathagu JN, Sang JK, Maina CW (2018) Modelling the impacts of structural conservation measures on sediment and water yield in Thika-Chania catchment. Kenya Int Soil Water Conserv Res 6:165–174
Gebremicael TG, Mohamed YA, Betrie GD, van der Zaag P, Teferi E (2013) Trend analysis of runoff and sediment fluxes in the Upper Blue Nile basin: a combined analysis of statistical tests, physically-based models and land use maps. J Hydrol 482:57–68
Hengl T, de Jesus JM, Heuvelink GBM, Gonzalez MR, Kilibarda M, Blagotić A, Shangguan W, Wright MN, Geng X, Bauer-Marschallinger B, Guevara MA, Vargas R, MacMillan RA, Batjes NH, Leenaars JGB, Ribeiro E, Wheeler I, Mantel S, Kempen B (2017) SoilGrids250m: Global gridded soil information based on machine learning. PLOS ONE 12:e0169748
Himanshu SK, Pandey A, Yadav B, Gupta A (2019) Evaluation of best management practices for sediment and nutrient loss control using SWAT model. Soil Tillage Res 192:42–58
Hurni H (1985) Erosion-productivity-conservation systems in Ethiopia. In: proceedings of paper presented at the 4th international conference on soil conservation, Maracay, Venezuela.
Hurni H, Tato K, Zeleke G (2005) The implications of changes in population, land use, and land management for surface runoff in the Upper Nile basin area of Ethiopia. Mt Res Dev 25(2):147–154
Jembere K, Mamo T, Kibret K (2017) Characteristics of agricultural landscape features and local soil fertility management practices in Northwestern Amhara, Ethiopia. J Agron 16:180–195
Lal R (1994) Water management in various crop production systems related to soil tillage. Soil Tillage Res 30:169–185
Lam QD, Schmalz B, Fohrer N (2011) The impact of agricultural Best Management Practices on water quality in a North German lowland catchment. Environ Monit Assess 183:351–379
Lamba J, Thompson AM, Karthikeyan KG, Panuska JC, Good LW (2016) Effect of best management practice implementation on sediment and phosphorus load reductions at sub-watershed and watershed scale using SWAT model. Int J Sediment Res 31:386–394
Lemma H, Admasu T, Dessie M, Fentie D, Deckers J, Frankl A, Poesen J, Adgo E, Nyssen J (2018) Revisiting lake sediment budgets: How the calculation of lake lifetime is strongly data and method dependent. Earth Surf Process Landf 43(3):593–607
Lemma H, Frankl A, van Griensven A, Poesen J, Adgo E, Nyssen J (2019) Identifying erosion hotspots in Lake Tana Basin from a multisite Soil and Water Assessment Tool validation: opportunity for land managers. Land Degrad Dev 30:1449–1467
López-Ballesteros A, Senent-Aparicio J, Srinivasan R, Pérez-Sánchez J (2019) Assessing the Impact of Best Management Practices in a Highly Anthropogenic and Ungauged Watershed Using the SWAT Model: a Case Study in the El Beal Watershed (Southeast Spain). Agronomy 9:576
Mekonnen M, Keesstra SD, Ritsema CJ, Stroosnijder L, Baartman JEM (2016) Sediment trapping with indigenous grass species showing differences in plant traits in northwest Ethiopia. Catena 147:755–763
Melaku ND, Renschler CS, Flagler J, Bayu W, Klik A (2018) Integrated impact assessment of soil and water conservation structures on runoff and sediment yield through measurements and modeling in the Northern Ethiopian Highlands. Catena 169:140–150
Merriman KR, Daggupati P, Srinivasan R, Hayhurst B (2019) Assessment of site-specific agricultural Best Management Practices in the Upper East River watershed, Wisconsin, using a field-scale SWAT model. J Gt Lakes Res 45:619–641
Monserud R (1990) Methods for comparing global vegetation maps, Report WP-90-40. IIASA, Laxenburg
Moriasi D, Arnold J, Van Liew M, Bingner R, Harmel R, Veith T (2007) Model evaluation guidelines for systematic quantification of accuracy in watershed simulations. Trans ASABE 50(3):885–900
MoWIE (2019) Source of streamflow and sediment data: the Ethiopian Ministry of Water, Irrigation and Electricity (MoWIE). Addis Ababa, Ethiopia
Nie W, Yuan Y, Kepner W, Nash M, Jackson M, Erickson C (2011) Assessing impacts of Land use and Land cover changes on hydrology for the upper San Pedro watershed. J Hydrol 407:105–114
NMSA (2019) Source of climate data: the Ethiopian National Meteorological Services Agency (NMSA). Addis Ababa, Ethiopia
Nyssen J, Poesen J, Gebremichael D, Vancampenhout K, D'aes M, Yihdego G, Govers G, Leirs H, Moeyersons J, Naudts J, Haregeweyn N, Haile M, Deckers J (2007a) Interdisciplinary on-site evaluation of stone bunds to control soil erosion on cropland in Northern Ethiopia. Soil Tillage Res 94:151–163
Nyssen J, Poesen J, Moeyersons J, Haile M, Deckers J (2007b) Dynamics of soil erosion rates and controlling factors in the Northern Ethiopian Highlands-towards a sediment budget. Earth Surf Process Landforms https://doi.org/10.1002/esp.1569
Oldeman LR, van Lynden GWJ, van Engelen VWP (1995) An international methodology for soil degradation assessment and for a soils and terrain digital database (SOTER). In: Paper presented at the regional workshop on assessment and monitoring of land degradation, Cairo, May 13–15, 1995. International Soil Reference and Information Center (ISRIC)
Park JY, Yu YS, Hwang SJ, Kim C, Kim SJ (2014) SWAT modeling of best management practices for Chungju dam watershed in South Korea under future climate change scenarios. Paddy Water Environ https://doi.org/10.1007/s10333-014-0424-4
Pimentel D (2006) Soil erosion: a food and environmental treat. Environ Dev Sustain 8:119–137
Pimentel D, Burgess M (2013) Soil erosion threatens food production. Agriculture 3:443–463
Reusing M, Schneider T, Ammer U (2000) Modeling soil loss rates in the Ethiopian highlands by integration of high resolution MOMS-02/D2-stereo-data in a GIS. Int J Remote Sens 21(9):1885–1896

Rocha J, Duarte A, Silva M, Fabres S, Vasques J, Revilla-Romero B, Quintela A (2020) The Importance of High Resolution Digital Elevation Models for Improved Hydrological Simulations of a Mediterranean Forested Catchment. Remote Sens 12:3287. https://doi.org/10.3390/rs12203287

Saxton K, Rawls W (2006) Soil water characteristic estimates by texture and organic matter for hydrologic solutions. Soil Sci Soc Am J 70:1569–1578

Setegn S, Srinivasan R, Dargahi B (2008) Hydrological modelling in the Lake Tana basin, Ethiopia using SWAT model. Open Hydrol J 2:49–62

Setegn SG, Dargahi B, Srinivasan R, Melesse AM (2010) Modeling of sediment yield from Anjeni-Gauged watershed, Ethiopia using SWAT model. JAWRA 46(3):514–526

Setegn SG, Srinivasan R, Dargahi B, Melesse AM (2009) Spatial delineation of soil erosion vulnerability in the Lake Tana basin, Ethiopia. Hydrol Process https://doi.org/10.1002/hyp.7476

Sonneveld BGJS, Keyzer MA (2003) Land under pressure: soil conservation concerns and opportunities for Ethiopia. Land Degrad Dev 14:5–23

Speth JG (1994) Towards an effective and operational international convention on desertification. International Convention on Desertification, Int. Negotiating Comm, United Nations, New York, NY

SRTM (2019) Source of the 30m resolution Shuttle Radar Topography Mission (STRM) Digital Elevation Model (DEM). https://earthexplorer.usgs.gov/(accessed 12.9.2019).

Taddese G (2001) Land degradation: a challenge to Ethiopia. Environ Manag 27(6):815–824

Tamene L, Adimassu Z, Aynekulu E, Yaekob T (2017) Estimating landscape susceptibility to soil erosion using a GIS-based approach in Northern Ethiopia. Int Soil Water Conserv Res 5:221–230

Temesgen H, Nyssen J, Zenebe A, Haregeweyn N, Kindu M, Lemenih M, Haile M (2013) Ecological succession and land use changes in a lake retreat area (Main Ethiopian Rift Valley). J Arid Environ 91:53–60

Tigabu TB, Wagner PD, H"rmann G, Fohrer N(2019) Modeling the impact of agricultural crops on the spatial and seasonal variability of water balance components in the Lake Tana basin, Ethiopia. Hydrol Res 50:1376–1396

Uhlenbrook S, Mohamed Y, Gragne A (2010) Analyzing catchment behavior through catchment modeling in the Gilgel Abay, Upper Blue Nile River Basin, Ethiopia. Hydrol Earth Syst Sci 14:2153–2165

Uniyal B, Jha MK, Verma AK, Anebagilu PK (2020) Identification of critical areas and evaluation of best management practices using SWAT for sustainable watershed management. Sci Total Environ 744:140737

USDA-SCS (United States Department of Agriculture–Soil Conservation Service) (1972) National Engineering Handbook, Section 4 Hydrology. USDA, Washington, DC

USGS (2019) Source of the 2001 Landsat_7 ETM: The United States Geological Survey (USGS). https://earthexplorer.usgs.gov/ (accessed 27.10.2019)

Waidler D, White M, Steglich E, Wang S, Williams J, Jones CA, Srinivasan R (2011) Guide for SWAT and APEX. Texas Water Resources Institute Technical Report No. 399. Texas A&M University System, College Station, Texas, p 77843–2118

Welde K (2016) Identification and prioritization of subwatersheds for land and water management in Tekeze dam watershed. North Ethiop Int Soil Water Conserv Res 4:30–38

Williams JR (1995) Chapter 25: The EPIC model. In V.P. Singh (ed) Computer models of watershed hydrology. Water Resources Publications. p 909–1000

Wolancho KW (2012) Watershed management: an option to sustain Dam and Reservoir function in Ethiopia. J Environ Sci Technol 5 (5):262–273

Worqlul AW, Ayana EK, Yen H, Jeong J, MacAlister C, Taylor R, Gerik TJ, Steenhuis TS (2018) Evaluating hydrologic responses to soil characteristics using SWAT model in a paired-watersheds in the Upper Blue Nile Basin. Catena 163:332–341

Yihenew G, Yihenew B (2013) Costs of nutrient losses in priceless soils eroded from the highlands of Northwestern Ethiopia. J Agric Sci 5(7):1916–9752

Yohannes F (2005) Soil erosion and sedimentation: The case of Lake Alemaya. In: proceedings of the second awareness creation workshop on wetlands in the Amhara Region, Ethiopia Wetlands and Natural Resources Association, Addis Ababa, pp 26–36

Zeleke G (2000) Landscape dynamics and soil erosion process modelling in the north-western Ethiopian highlands. PhD Thesis. Bern University, Bern

Zhang JX, Chang K, Wu JQ (2008) Effects of DEM resolution and source on soil erosion modelling: a case study using the WEPP model. Int J Geogr Inf Sci 22(8):925–942